

Electronic Supporting Information

**Low Coordinate Iron Derivatives Stabilized by a β -Diketiminate Mimic. Synthesis and
Coordination Chemistry of Enamidophosphinimine Scaffolds to Generate Diiron
Dinitrogen Complexes**

Nicholas M. Hein, Tatsuya Suzuki, Takahiko Ogawa, and Michael D. Fryzuk*

Department of Chemistry

The University of British Columbia

2036 Main Mall

Vancouver, BC, CANADA

V6T 1Z1

Contents:

X-ray Diffraction Data.....	2
NMR Spectra.....	11
Mössbauer Spectrum.....	41

X-ray crystallographic data and collection parameters

Table S1: Crystal data and structure refinement for **4a**

Identification code	mf1117a	
Empirical formula	$C_{35}H_{54}N_2PFeBr$	
Formula weight	669.53	
Temperature	90K	
Crystal size	$0.2 \times 0.18 \times 0.18 \text{ mm}^3$	
Radiation	MoK α ($\lambda = 0.71069 \text{ \AA}$)	
Crystal system	orthorhombic	
Space group	Pbca	
Unit cell dimensions	$a=17.3586(5) \text{ \AA}$	$\alpha=90^\circ$
	$b=16.9214(5) \text{ \AA}$	$\beta=90^\circ$
	$c=23.4188(7) \text{ \AA}$	$\gamma=90^\circ$
Volume	$6878.8(4) \text{ \AA}^3$	
Z	8	
Density (calculated)	1.293 g/cm^3	
Absorption Coefficient	1.672 mm^{-1}	
F(000)	2832.0	
2 θ range for data collection	3.478 to 55.02 $^\circ$	
Index ranges	$-22 \leq h \leq 15, -21 \leq k \leq 18, -24 \leq l \leq 30$	
Reflections collected	34340	
Independent reflections	$7900 [R_{\text{int}} = 0.0476, R_{\text{sigma}} = 0.0481]$	
Data/restraints/parameters	7900/0/373	
Completeness to θ	99.8%	
Goodness-of-fit on F^2	1.038	
Final R indexes [$I \geq 2\sigma(I)$]	$R_1 = 0.0528, wR_2 = 0.1149$	
Final R indexes [all data]	$R_1 = 0.0814, wR_2 = 0.1265$	
Largest diff. peak/hole	$2.57/-2.34 \text{ e\AA}^{-3}$	

Table S2: Crystal data and structure refinement for **4b**

Identification code	mf1189	
Empirical formula	$C_{27}H_{38}BrFeN_2P$	
Formula weight	557.32	
Temperature	90K	
Crystal size	$0.09 \times 0.08 \times 0.04 \text{ mm}^3$	
Radiation	MoK α ($\lambda = 0.71069 \text{ \AA}$)	
Crystal system	triclinic	
Space group	P-1	
Unit cell dimensions	$a=13.121(3) \text{ \AA}$	$\alpha=90.837(4)^\circ$
	$b=15.896(4) \text{ \AA}$	$\beta=109.446(4)^\circ$
	$c=16.706(4) \text{ \AA}$	$\gamma=101.917(4)^\circ$
Volume	$3201.6(14) \text{ \AA}^3$	
Z	4	
Density (calculated)	1.156 g/cm^3	
Absorption Coefficient	1.783 mm^{-1}	
F(000)	1160.0	
2 θ range for data collection	2.596 to 53.036 $^\circ$	
Index ranges	$-16 \leq h \leq 16, -19 \leq k \leq 19, -20 \leq l \leq 20$	
Reflections collected	44303	
Independent reflections	13084 [$R_{\text{int}} = 0.1318, R_{\text{sigma}} = 0.1376$]	
Data/restraints/parameters	13084/0/545	
Completeness to θ	98.5%	
Goodness-of-fit on F^2	0.909	
Final R indexes [$I \geq 2\sigma(I)$]	$R_1 = 0.0827, wR_2 = 0.2030$	
Final R indexes [all data]	$R_1 = 0.1452, wR_2 = 0.2298$	
Largest diff. peak/hole	$2.17/-1.04 \text{ e\AA}^{-3}$	

Table S3: Crystal data and structure refinement for **4c**

Identification code	mf1098	
Empirical formula	$C_{64}H_{96}N_4P_2Fe_2Br_2$	
Formula weight	1254.90	
Temperature	90K	
Crystal size	$0.16 \times 0.13 \times 0.02 \text{ mm}^3$	
Radiation	MoK α ($\lambda = 0.71069 \text{ \AA}$)	
Crystal system	triclinic	
Space group	P-1	
Unit cell dimensions	$a=9.999(3) \text{ \AA}$	$\alpha=62.101(6)^\circ$
	$b=13.544(5) \text{ \AA}$	$\beta=72.296(7)^\circ$
	$c=13.905(5) \text{ \AA}$	$\gamma=85.151(7)^\circ$
Volume	$1581.7(9) \text{ \AA}^3$	
Z	1	
Density (calculated)	1.317 g/cm^3	
Absorption Coefficient	1.813 mm^{-1}	
F(000)	660.0	
2θ range for data collection	3.41 to 54.974°	
Index ranges	$-12 \leq h \leq 12, -17 \leq k \leq 17, -18 \leq l \leq 18$	
Reflections collected	24646	
Independent reflections	7109 [$R_{\text{int}} = 0.0767, R_{\text{sigma}} = 0.0838$]	
Data/restraints/parameters	7109/0/345	
Completeness to θ	99.2%	
Goodness-of-fit on F^2	1.074	
Final R indexes [$I \geq 2\sigma(I)$]	$R_1 = 0.0670, wR_2 = 0.1588$	
Final R indexes [all data]	$R_1 = 0.1023, wR_2 = 0.1715$	
Largest diff. peak/hole	$1.57/-0.67 \text{ e\AA}^{-3}$	

Table S4: Crystal data and structure refinement for **5a**

Identification code	mf1148	
Empirical formula	$C_{70}H_{108}N_6P_2Fe_2$	
Formula weight	1207.26	
Temperature	90 K	
Crystal size	$0.1 \times 0.08 \times 0.03$ mm ³	
Radiation	MoK α ($\lambda = 0.71069$ Å)	
Crystal system	monoclinic	
Space group	P2 ₁ /c	
Unit cell dimensions	$a=10.3990(6)$ Å	$\alpha=90^\circ$
	$b=28.6698(15)$ Å	$\beta=100.9200(10)^\circ$
	$c=22.9617(13)$ Å	$\gamma=90^\circ$
Volume	$6721.8(6)$ Å ³	
Z	4	
Density (calculated)	1.193 g/cm ³	
Absorption Coefficient	0.523 mm ⁻¹	
F(000)	2608.0	
2 θ range for data collection	2.298 to 55.11°	
Index ranges	$-13 \leq h \leq 13, -37 \leq k \leq 20, -24 \leq l \leq 29$	
Reflections collected	62062	
Independent reflections	15498 [$R_{int} = 0.0760, R_{sigma} = 0.0902$]	
Data/restraints/parameters	15498/0/745	
Completeness to θ	99.7%	
Goodness-of-fit on F^2	1.001	
Final R indexes [$I \geq 2\sigma(I)$]	$R_1 = 0.0479, wR_2 = 0.0833$	
Final R indexes [all data]	$R_1 = 0.0986, wR_2 = 0.0965$	
Largest diff. peak/hole	0.48/-0.39 eÅ ⁻³	

Table S5: Crystal data and structure refinement for **5b**

Identification code	mf1203	
Empirical formula	$C_{46}H_{67}N_3P_2Fe$	
Formula weight	779.81	
Temperature	90 K	
Crystal size	$0.24 \times 0.03 \times 0.025 \text{ mm}^3$	
Radiation	MoK α ($\lambda = 0.71073 \text{ \AA}$)	
Crystal system	monoclinic	
Space group	P2 ₁ /n	
Unit cell dimensions	$a = 19.562(3) \text{ \AA}$	$\alpha = 90^\circ$
	$b = 11.2091(14) \text{ \AA}$	$\beta = 112.138(3)^\circ$
	$c = 20.674(3) \text{ \AA}$	$\gamma = 90^\circ$
Volume	$4199.1(9) \text{ \AA}^3$	
Z	4	
Density (calculated)	1.234 g/cm ³	
Absorption Coefficient	0.471 mm ⁻¹	
F(000)	1680.0	
2 θ range for data collection	2.444 to 55.158°	
Index ranges	$-25 \leq h \leq 24, -10 \leq k \leq 14, -26 \leq l \leq 26$	
Reflections collected	37081	
Independent reflections	9688 [$R_{\text{int}} = 0.1579, R_{\text{sigma}} = 0.1611$]	
Data/restraints/parameters	9688/0/483	
Completeness to θ	99.4%	
Goodness-of-fit on F^2	0.974	
Final R indexes [$I \geq 2\sigma(I)$]	$R_1 = 0.0807, wR_2 = 0.1703$	
Final R indexes [all data]	$R_1 = 0.1598, wR_2 = 0.2062$	
Largest diff. peak/hole	$1.23/-0.89 \text{ e\AA}^{-3}$	

Table S6: Crystal data and structure refinement for **5c**

Identification code	mf987
Empirical formula	C ₆₄ H _{93.15} Fe ₂ N ₆ P ₂
Formula weight	1120.23
Temperature	90 K
Crystal size	0.21 × 0.014 × 0.014 mm ³
Radiation	MoKα ($\lambda = 0.71069 \text{ \AA}$)
Crystal system	monoclinic
Space group	C ₂ /c
Unit cell dimensions	a=21.642(5) Å $\alpha=90^\circ$ b= 20.337(5) Å $\beta= 98.831(5)^\circ$ c= 16.105(5) Å $\gamma= 90^\circ$
Volume	7004(3) Å ³
Z	4
Density (calculated)	1.062 g/cm ³
Absorption Coefficient	0.498 mm ⁻¹
F(000)	2405.0
2θ range for data collection	2.764 to 50.8°
Index ranges	-24 ≤ h ≤ 26, -24 ≤ k ≤ 24, -19 ≤ l ≤ 19
Reflections collected	25483
Independent reflections	6423 [R _{int} = 0.0696, R _{sigma} = 0.0688]
Data/restraints/parameters	6423/0/362
Completeness to θ	99.6%
Goodness-of-fit on F ²	1.071
Final R indexes [I>=2σ (I)]	R ₁ = 0.0626, wR ₂ = 0.1623
Final R indexes [all data]	R ₁ = 0.0868, wR ₂ = 0.1704
Largest diff. peak/hole	1.25/-0.47 eÅ ⁻³

Table S7: Crystal data and structure refinement for **6**

Identification code	mf1134_a	
Empirical formula	$C_{35.5}H_{55.5}FeN_2P$	
Formula weight	597.14	
Temperature	90.15 K	
Crystal size	$0.52 \times 0.45 \times 0.41 \text{ mm}^3$	
Radiation	MoK α ($\lambda = 0.71069 \text{ \AA}$)	
Crystal system	monoclinic	
Space group	C ₂ /c	
Unit cell dimensions	$a = 26.340(3) \text{ \AA}$	$\alpha = 90^\circ$
	$b = 11.8226(16) \text{ \AA}$	$\beta = 106.786(3)^\circ$
	$c = 24.864(3) \text{ \AA}$	$\gamma = 90^\circ$
Volume	$7413.1(17) \text{ \AA}^3$	
Z	8	
Density (calculated)	1.070 g/cm ³	
Absorption Coefficient	0.473 mm ⁻¹	
F(000)	2588.0	
2 θ range for data collection	3.23 to 50.36°	
Index ranges	$-31 \leq h \leq 21, -14 \leq k \leq 14, -22 \leq l \leq 29$	
Reflections collected	51121	
Independent reflections	6599 [$R_{\text{int}} = 0.0389, R_{\text{sigma}} = 0.0248$]	
Data/restraints/parameters	6599/651/683	
Completeness to θ	99.0%	
Goodness-of-fit on F^2	1.065	
Final R indexes [$I \geq 2\sigma(I)$]	$R_1 = 0.1319, wR_2 = 0.3464$	
Final R indexes [all data]	$R_1 = 0.1487, wR_2 = 0.3532$	
Largest diff. peak/hole	$0.67/-1.76 \text{ e\AA}^{-3}$	

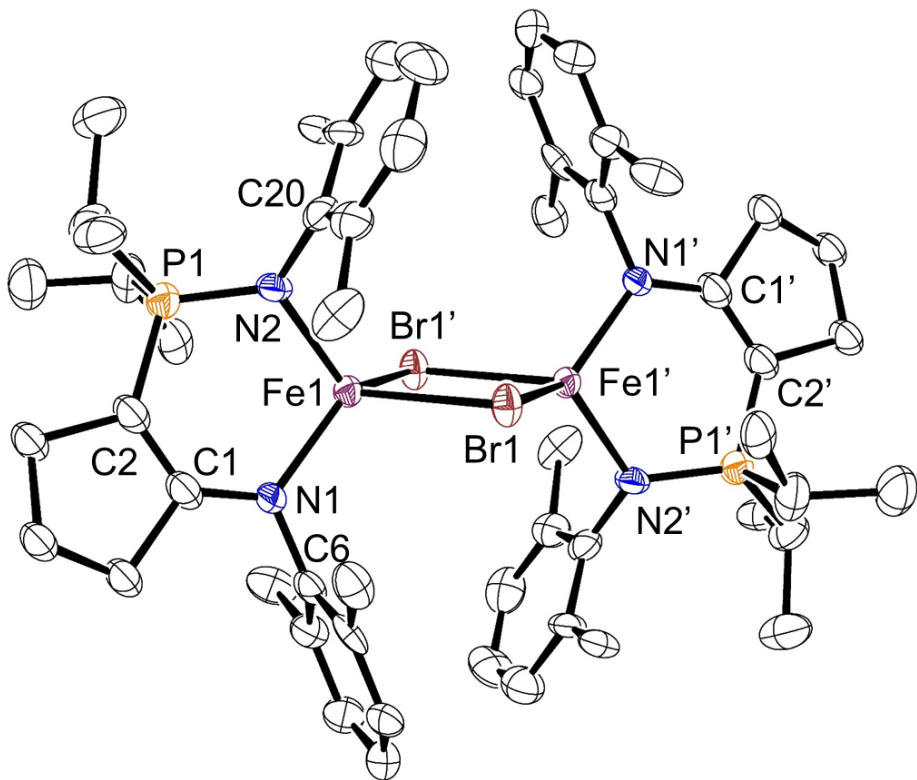


Figure S1: ORTEP drawing of the solid-state molecular structure of **4b** (ellipsoids at 50% probability level). All hydrogen atoms have been omitted for clarity. Selected bond lengths (\AA), angles (deg), and torsion angles (deg): C1-N1: 1.339(9), C1-C2: 1.358(11), C2-P1: 1.753(8), P1-N2: 1.645(6), N1-Fe1: 1.988(6), N2-Fe1: 2.009(6), Fe1-Br1: 2.5361(13), Fe1-Br1': 2.5415(13), Fe1-Fe1': 3.614(2), C1-N1-C6: 117.9(6), P1-N2-C20: 126.0(5), N1-Fe1-N2: 102.4(2), Br1-Fe1-Br1': 89.25(4), N1-Fe1-Br1: 112.08(17), N1-Fe1-Br1': 122.32(17), N2-Fe1-Br1: 114.42(18), N2-Fe1-Br1': 116.61(18), C1-C2-P1-N2: 25.8(9).

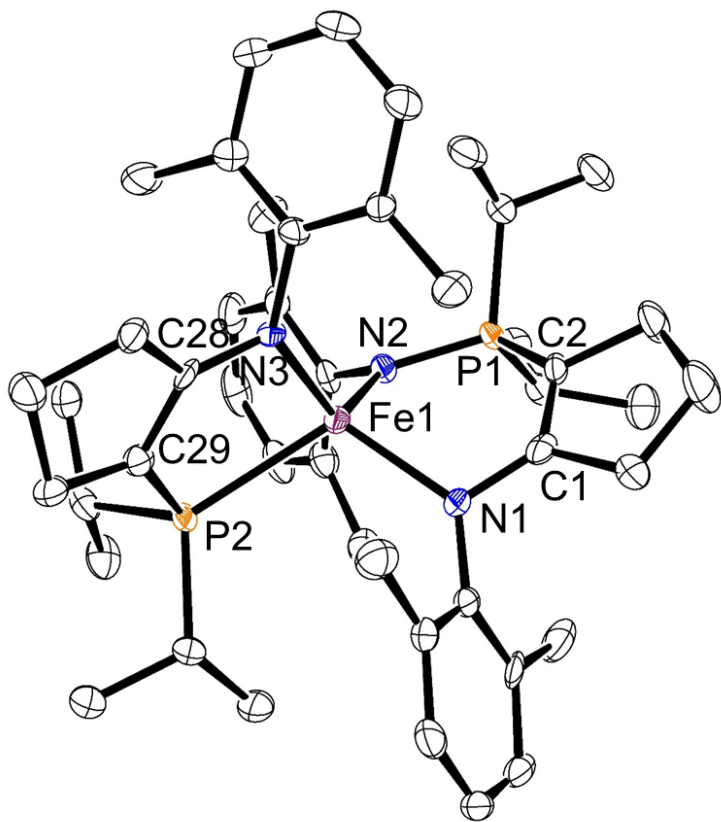


Figure S2: ORTEP drawing of the solid-state molecular structure of **5b** (ellipsoids at 50% probability level). All hydrogen atoms have been omitted for clarity. Selected bond lengths (Å), angles (deg): C1-N1: 1.368(5), C1-C2: 1.374(6), C2-P1: 1.747(5), P1-N2: 1.628(4), C28-N3: 1.359(5), C28-C29: 1.381(5), P2-C29: 1.772(4), N1-Fe1: 2.052(3), N2-Fe1: 2.023(4), N3-Fe1: 2.017(3), P2-Fe1: 2.4981(12), N1-Fe1-N2: 98.37(14), N2-Fe1-N3: 122.76(14), N1-Fe1-P2: 111.93(9), N3-Fe1-P2: 86.07(10).

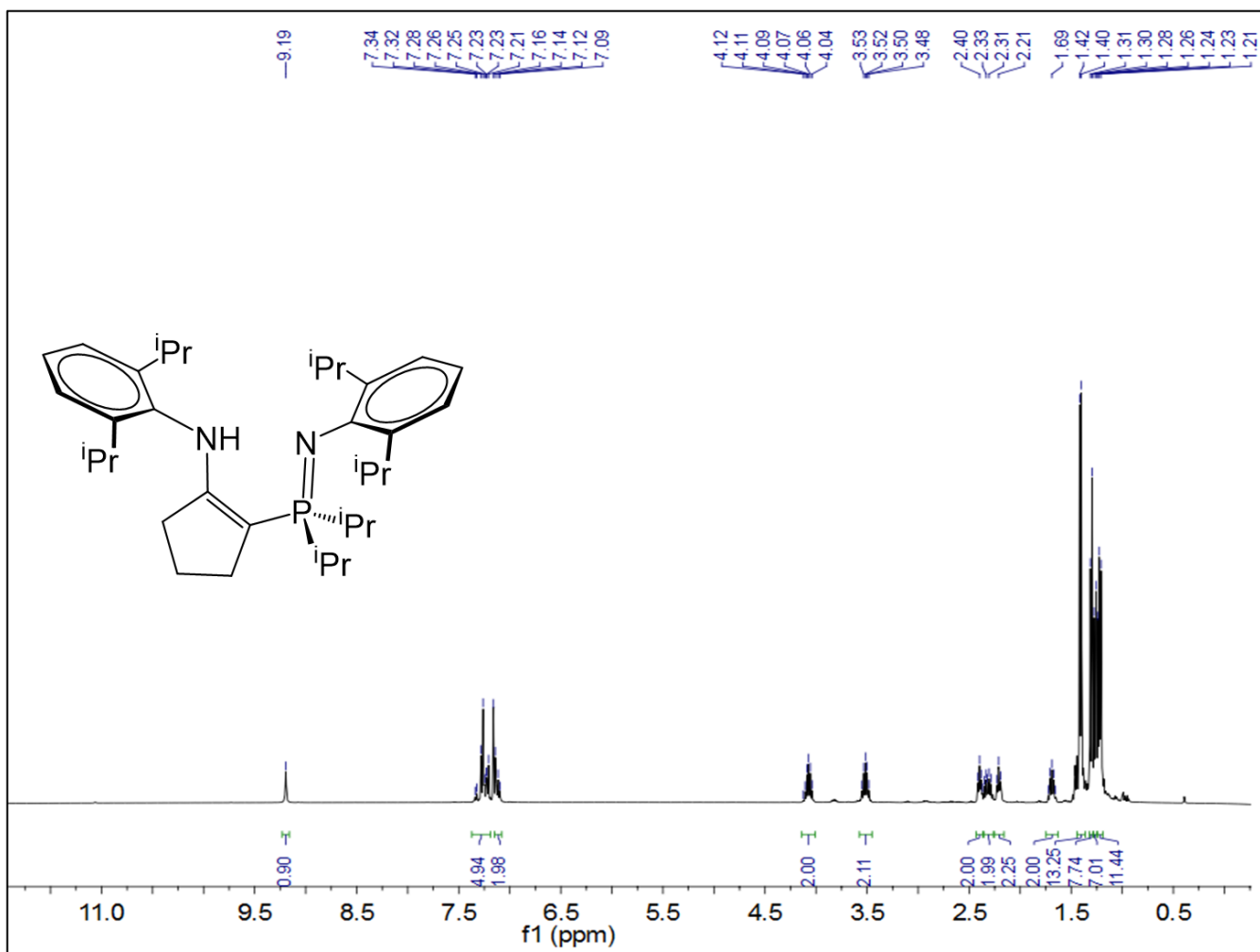


Figure S3: ^1H NMR spectrum for $[\text{^{CY5}NpN}^{\text{DIPP},\text{DIPP}}]\text{H 2a}$ (400 MHz, d_6 -benzene, 298 K).

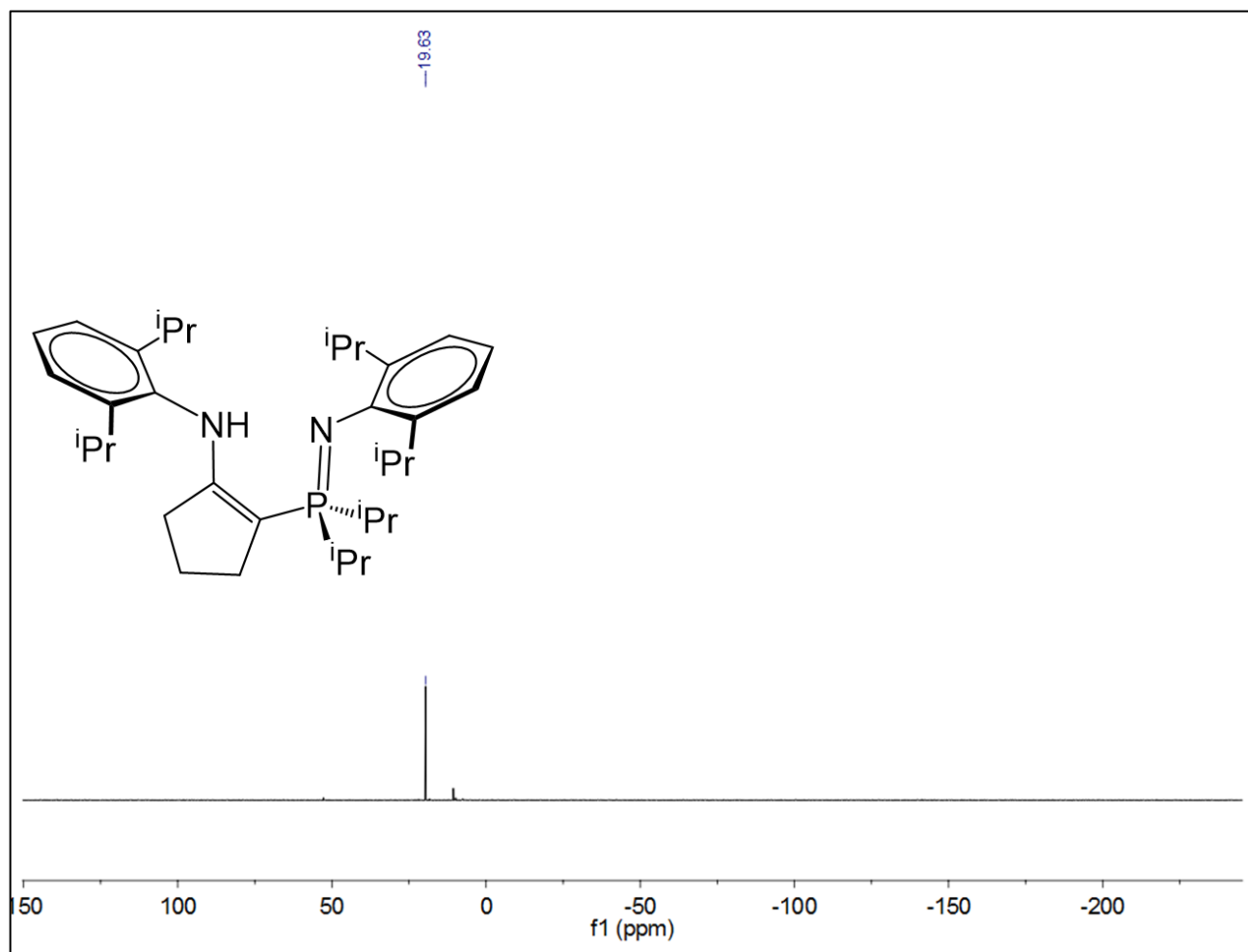


Figure S4: $^{31}\text{P}\{\text{H}\}$ NMR spectrum for $[\text{CY}^5\text{NpN}^{\text{DIPP},\text{DIPP}}]\text{H } \mathbf{2a}$ (161 MHz, d_6 -benzene, 298 K).

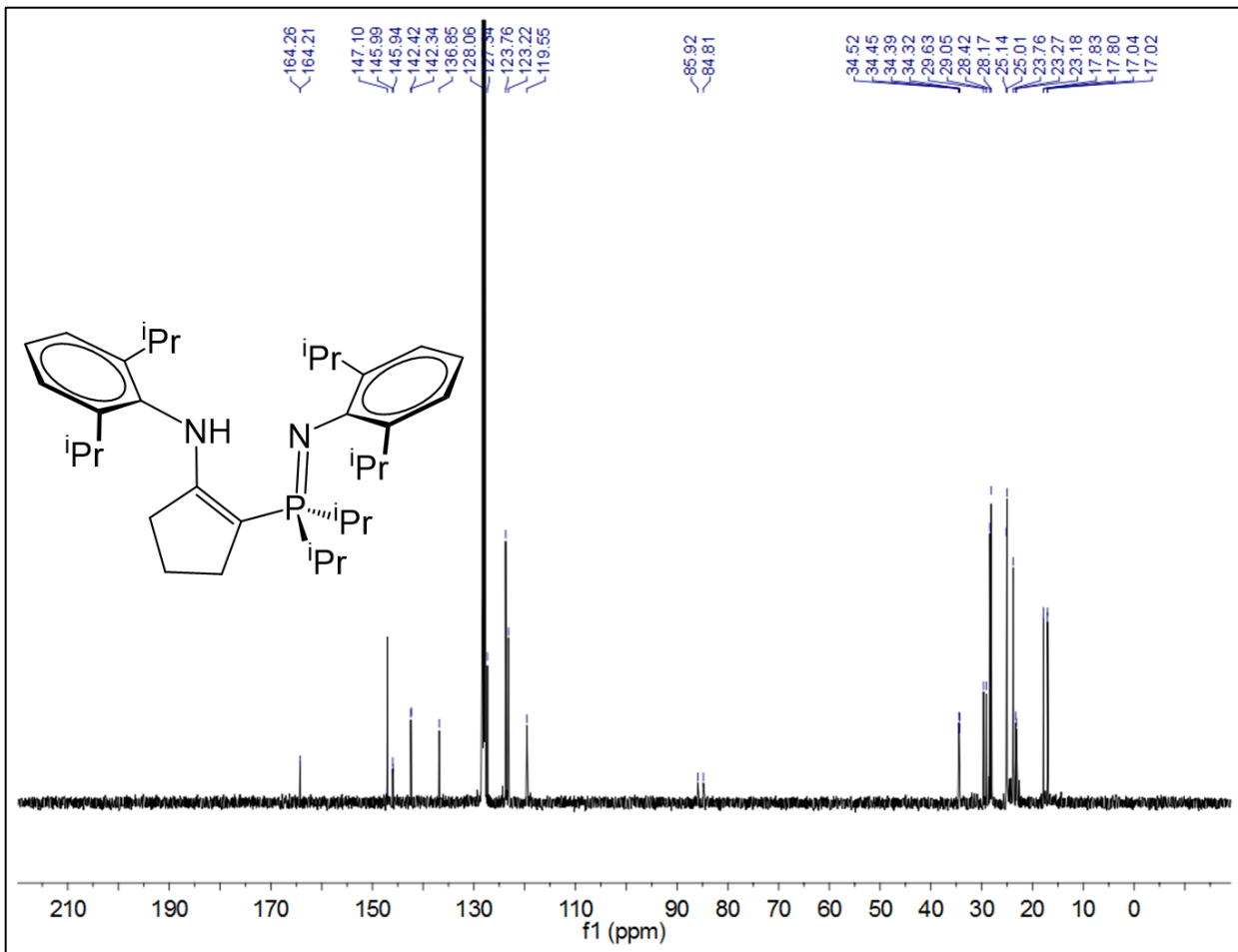


Figure S5: $^{13}\text{C}\{\text{H}\}$ NMR spectrum for $[\text{CY}^5\text{NpN}^{\text{DIPP},\text{DIPP}}]\text{H } \mathbf{2a}$ (101 MHz, d_6 -benzene, 298 K).

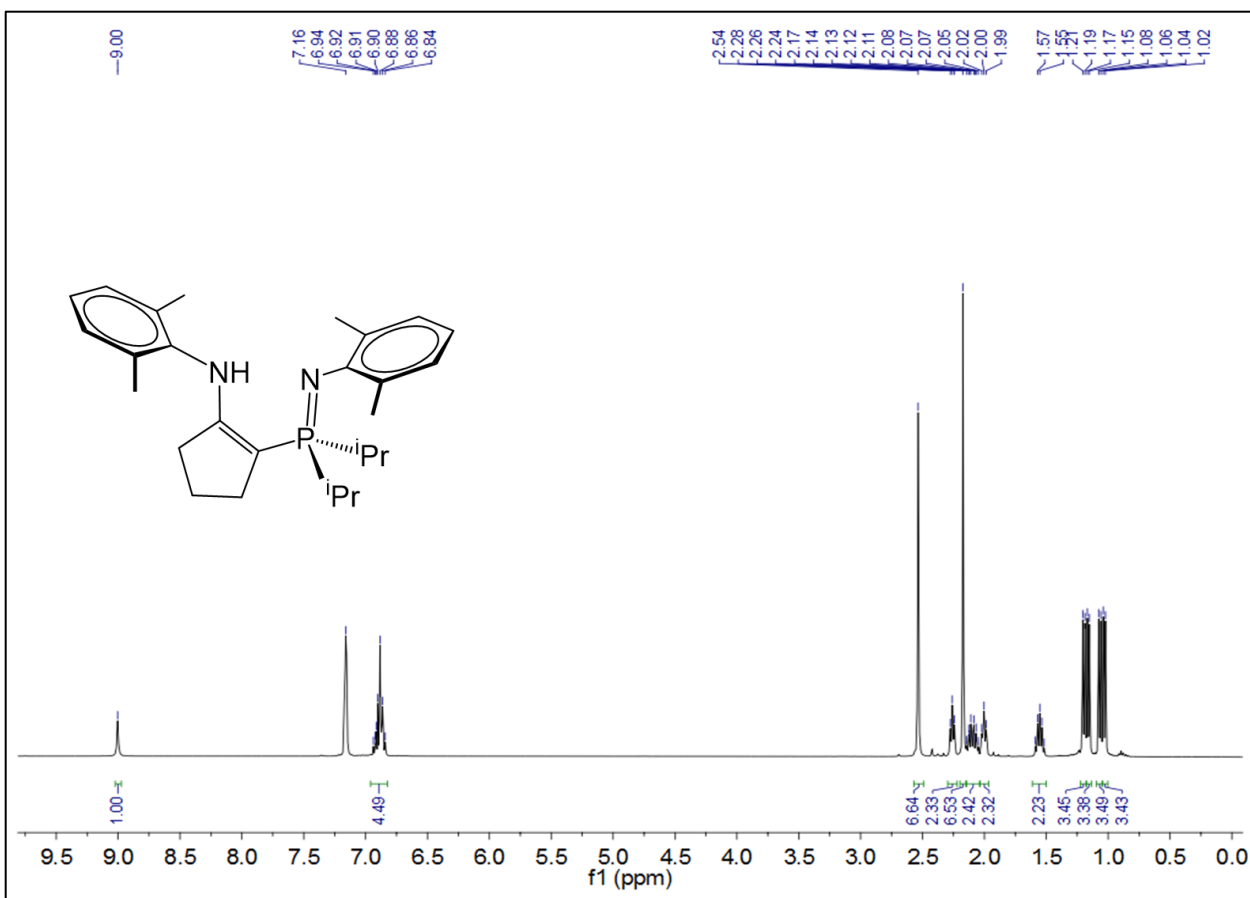


Figure S6: ^1H NMR spectrum for $[\text{CY}^5\text{NpN}^{\text{DMP},\text{DMP}}]\text{H } \mathbf{2b}$ (400 MHz, d_6 -benzene, 298 K).

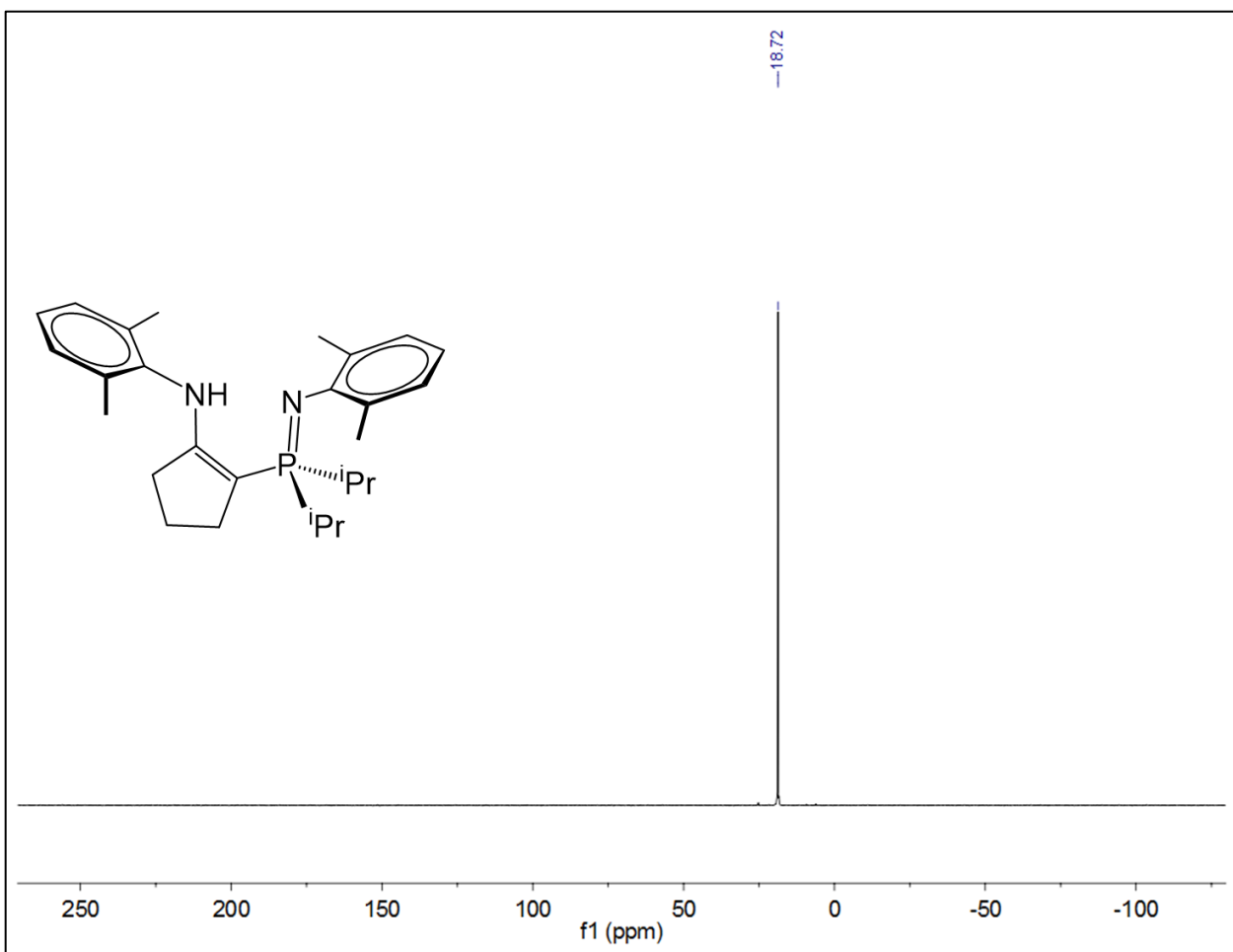


Figure S7: $^{31}\text{P}\{\text{H}\}$ NMR spectrum for $[{}^{\text{CY5}}\text{NpN}^{\text{DMP,DMP}}]\text{H } \mathbf{2b}$ (121 MHz, d_6 -benzene, 298 K).

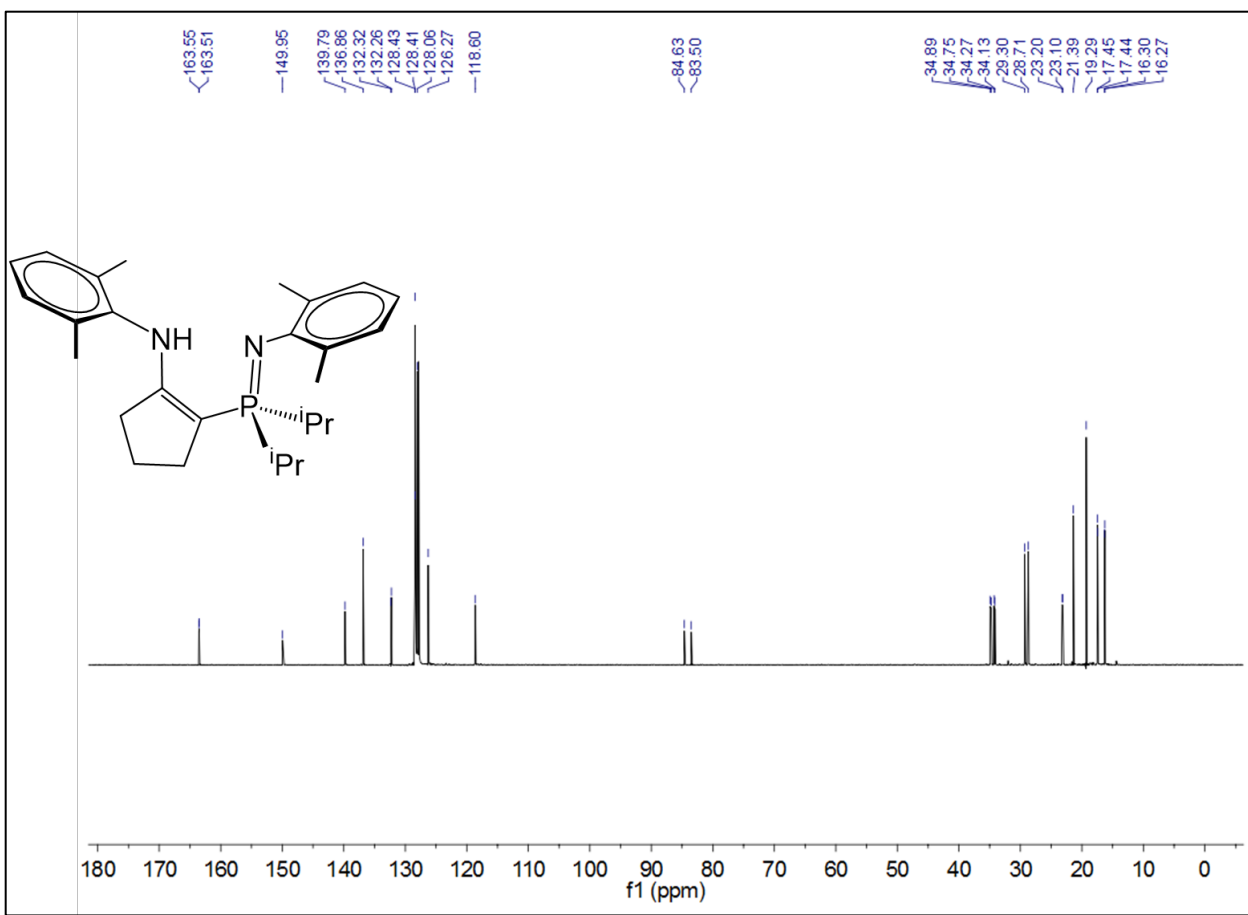


Figure S8: $^{13}\text{C}\{^1\text{H}\}$ NMR spectrum for $[\text{CY}^5\text{NpN}^{\text{DMP},\text{DMP}}]\text{H } \mathbf{2b}$ (101 MHz, d_6 -benzene, 298 K).

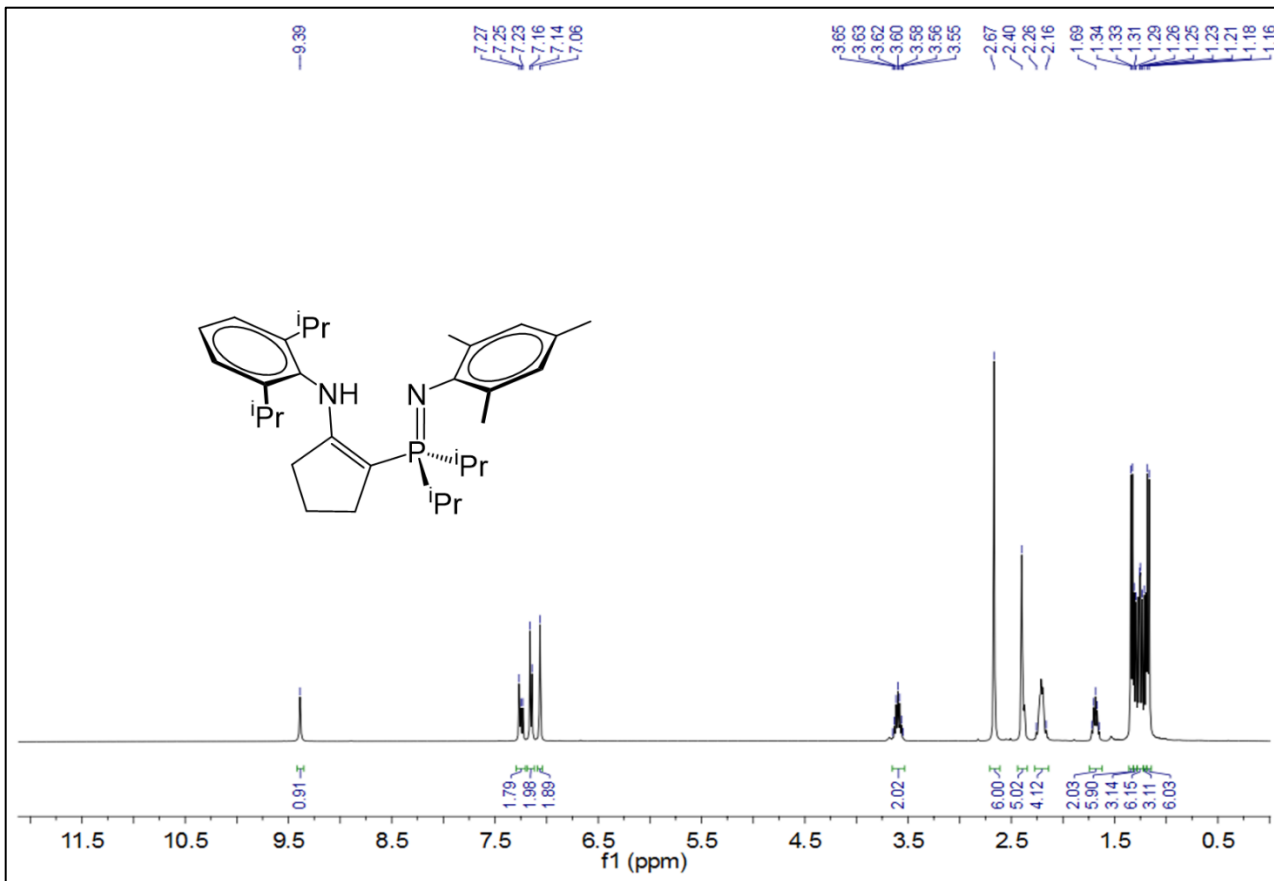


Figure S9: ^1H NMR spectrum for $[\text{CY}^5\text{NpN}^{\text{DIPP},\text{Mes}}]\text{H } \mathbf{2c}$ (400 MHz, d_6 -benzene, 298 K).

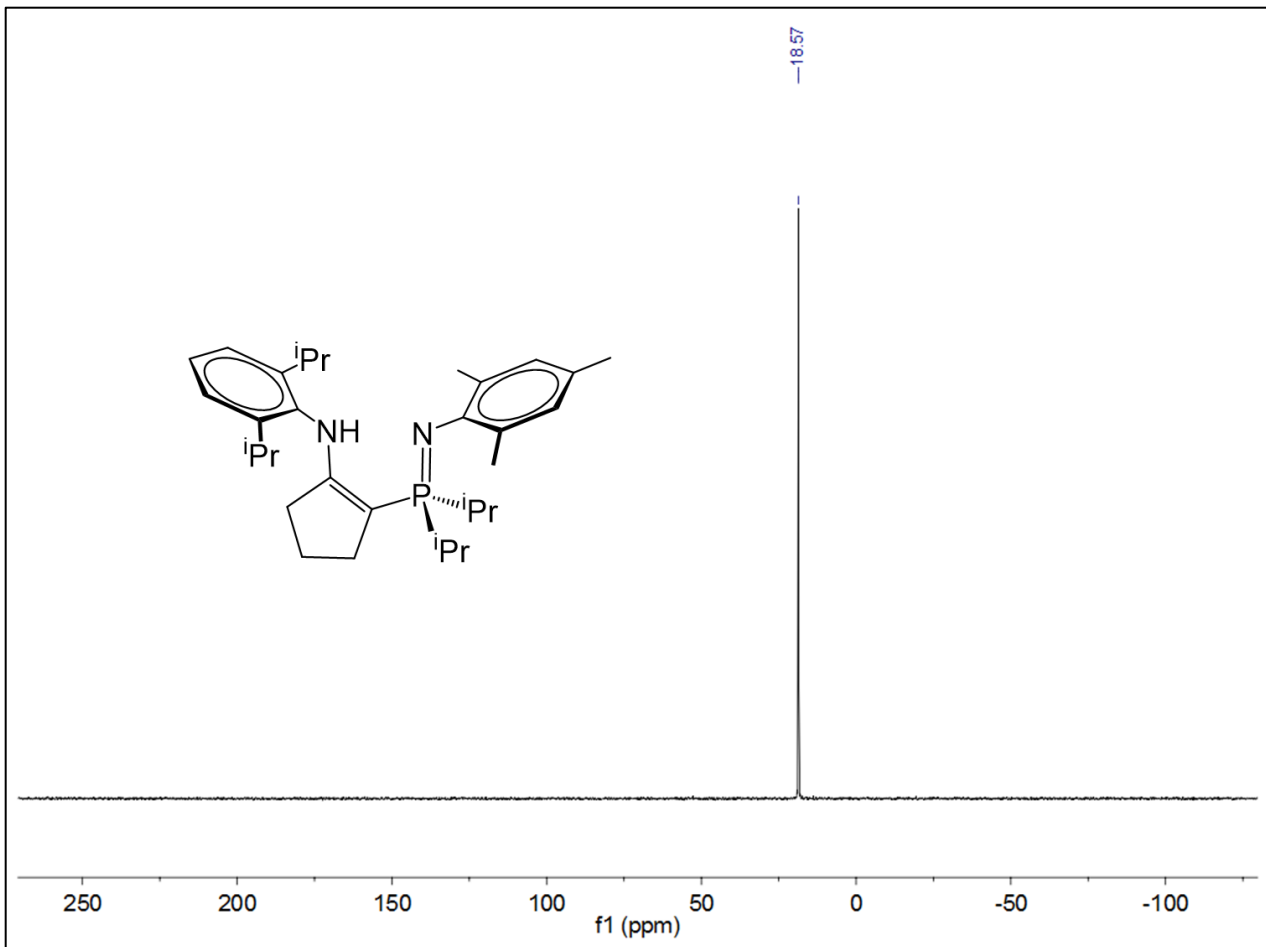


Figure S10: $^{31}\text{P}\{\text{H}\}$ NMR spectrum for $[\text{CY}^5\text{NpN}^{\text{DIPP},\text{Mes}}]\text{H}$ **2c** (121 MHz, d_6 -benzene, 298 K).

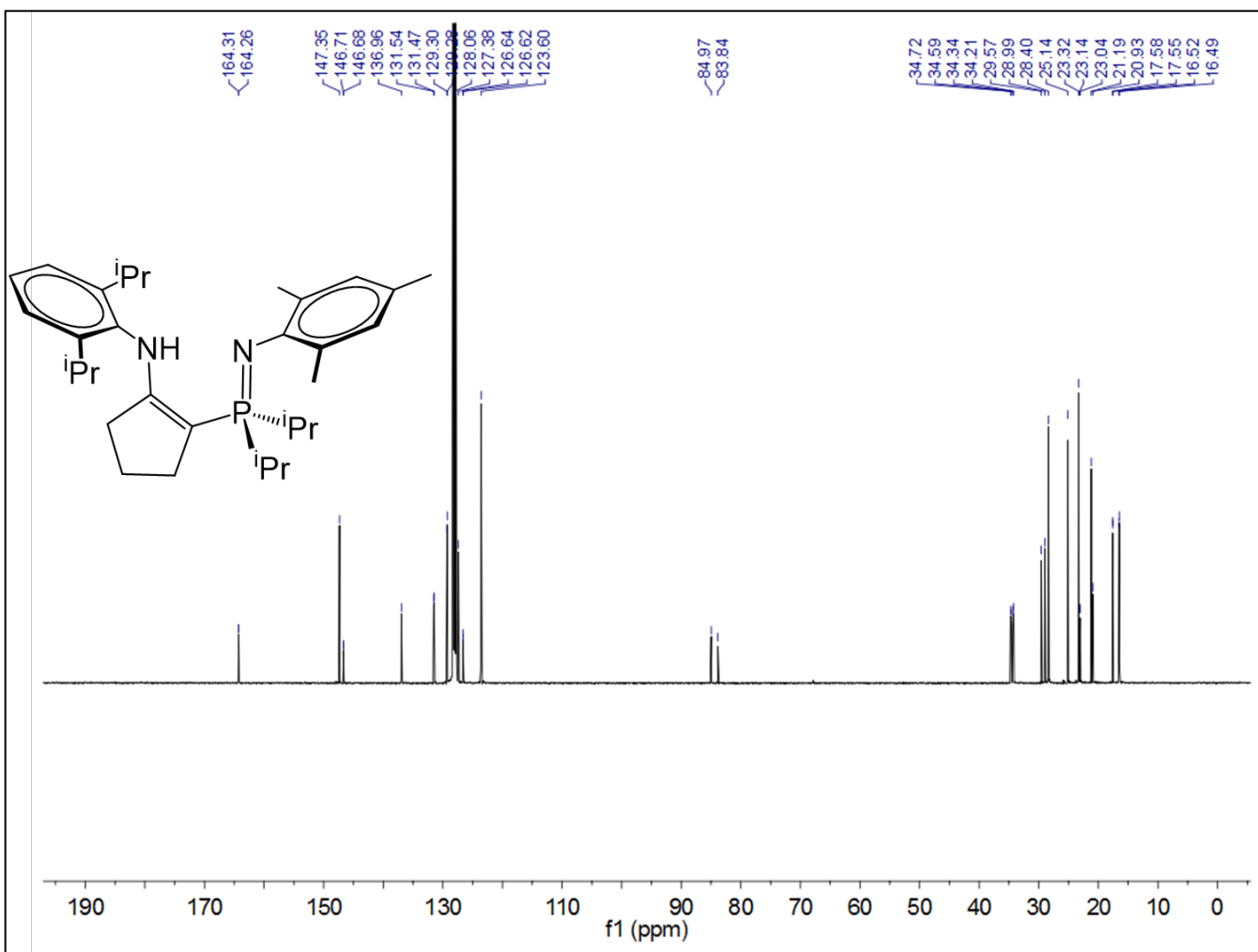


Figure S11: $^{13}\text{C}\{^1\text{H}\}$ NMR spectrum for $[\text{CY}^5\text{NpN}^{\text{DIPP},\text{Mes}}]\text{H } \mathbf{2c}$ (101 MHz, d_6 -benzene, 298 K).

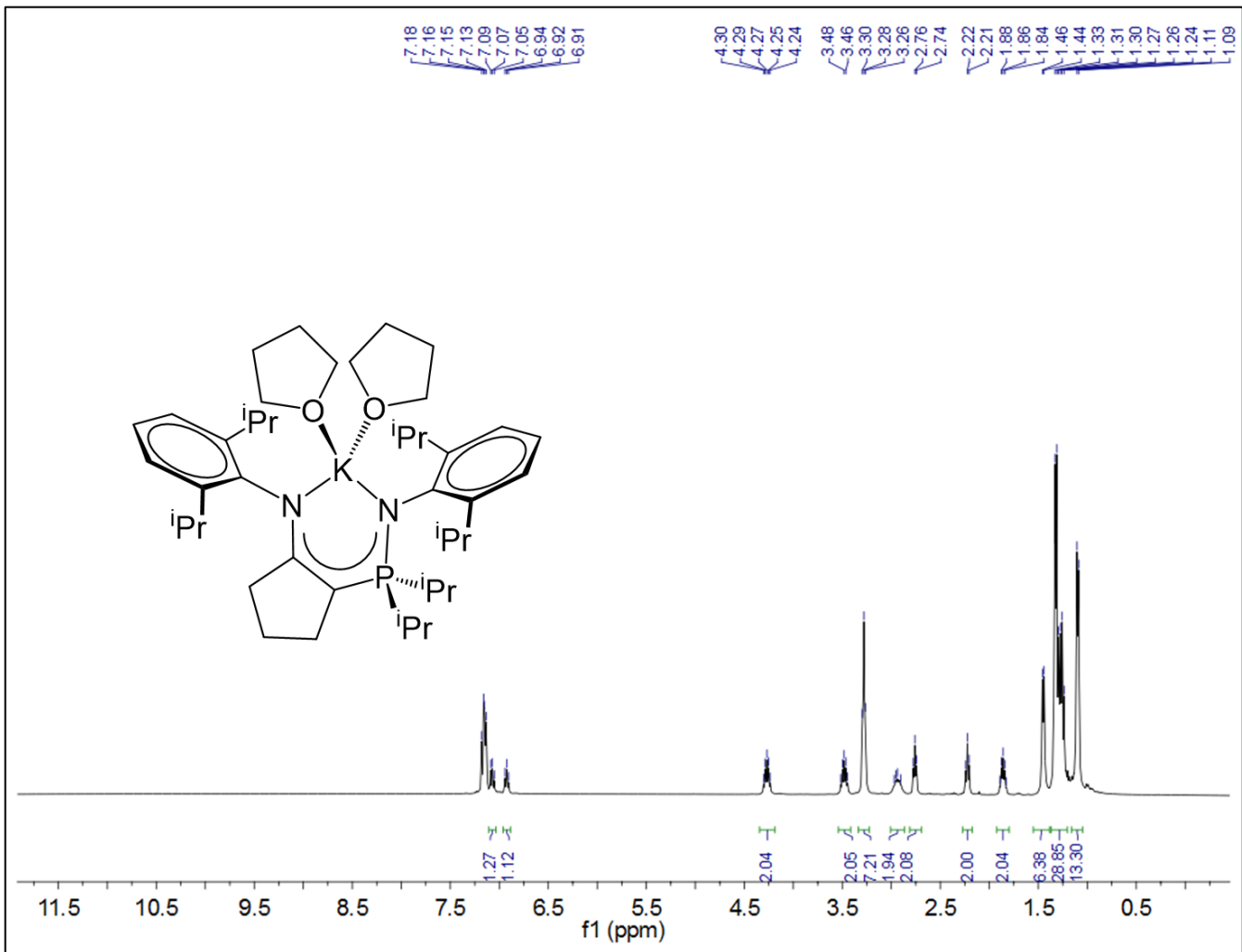


Figure S12: ^1H NMR spectrum for $[\text{CY}^5\text{NpN}^{\text{DIPP},\text{DIPP}}]\text{K}(\text{THF})_2 \mathbf{3a}$

(400 MHz, d_6 -benzene, 298 K).

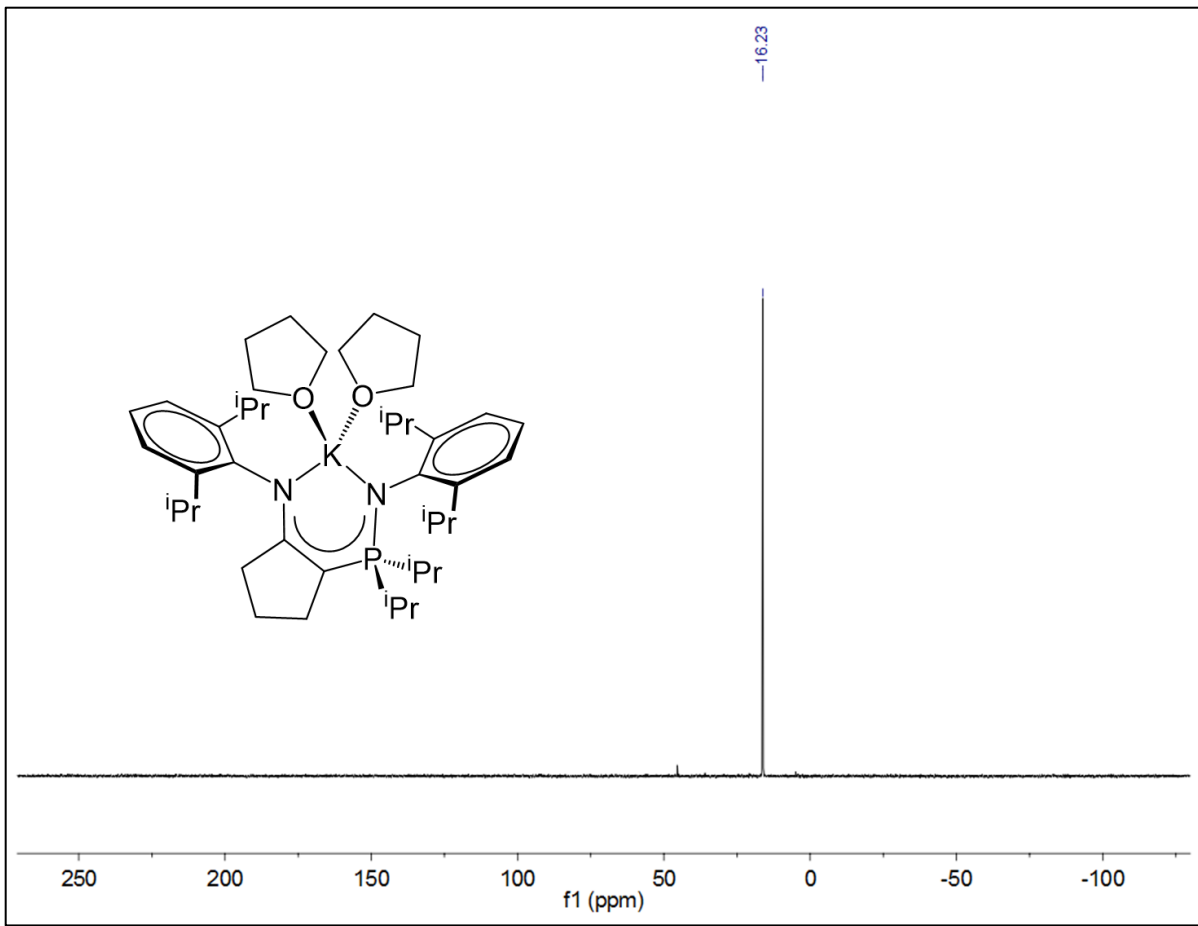


Figure S13: $^{31}\text{P}\{\text{H}\}$ NMR spectrum for $[\text{CY}^5\text{NpN}^{\text{DIPP},\text{DIPP}}]\text{K}(\text{THF})_2$ **3a**
(161 MHz, d_6 -benzene, 298 K).

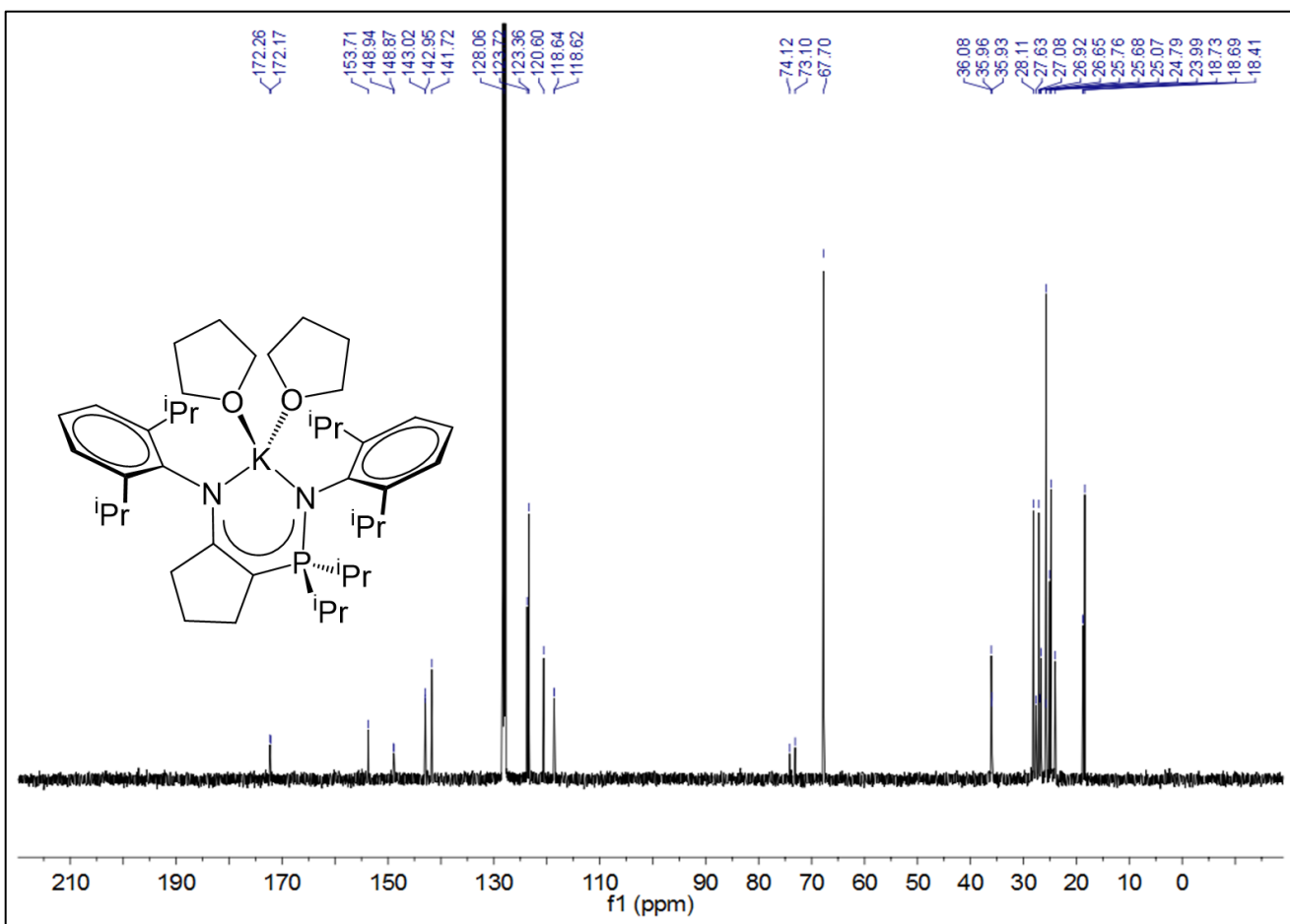


Figure S14: $^{13}\text{C}\{^1\text{H}\}$ NMR spectrum for $[\text{CY}^5\text{NpN}^{\text{DIPP},\text{DIPP}}]\text{K}(\text{THF})_2$ **3a**

(101 MHz, d_6 -benzene, 298 K).

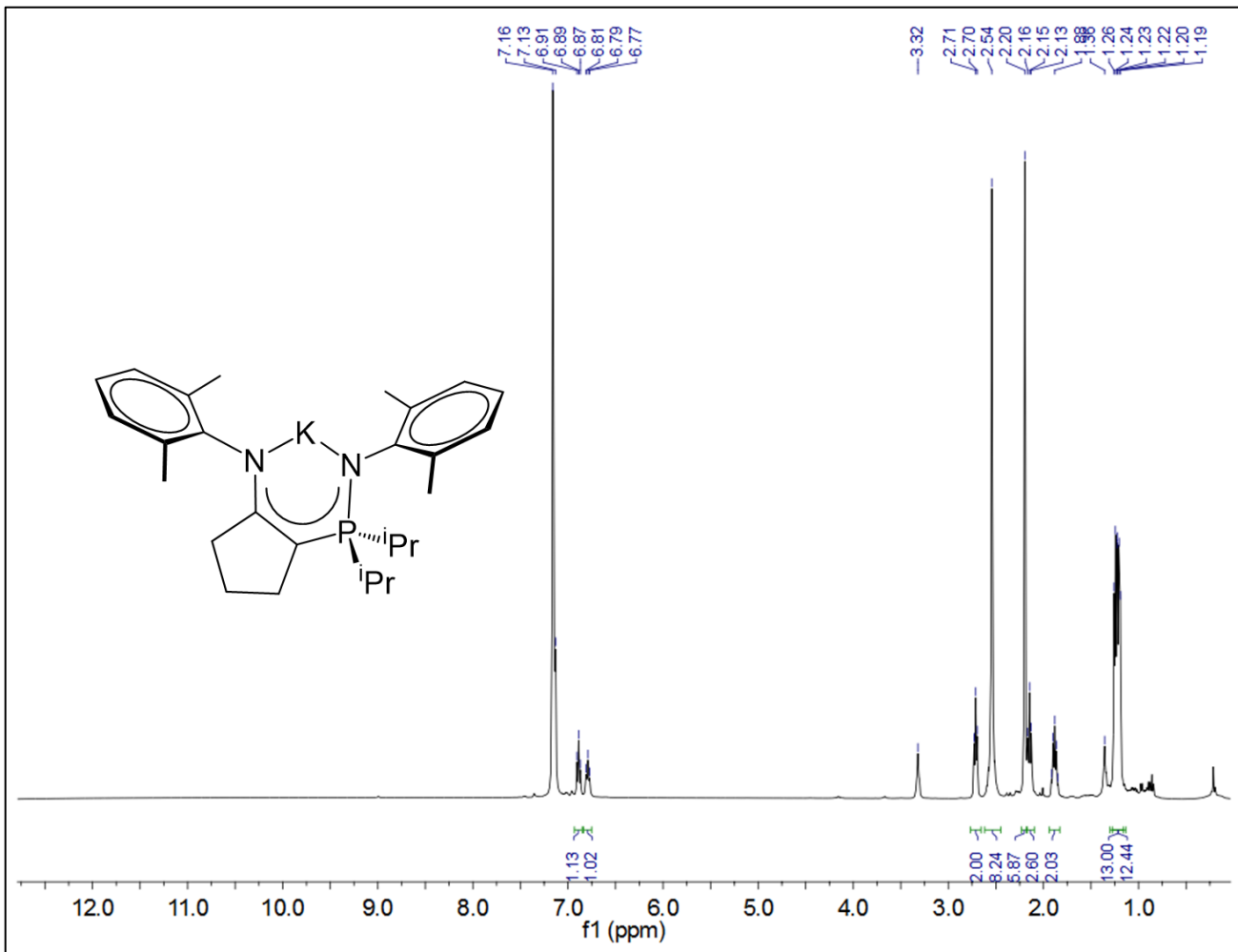


Figure S15: ^1H NMR spectrum for $[\text{CY}^5\text{NpN}^{\text{DMP},\text{DMP}}]\text{K}(\text{THF})_{0.25} \mathbf{3b}$
(400 MHz, d_6 -benzene, 298 K).

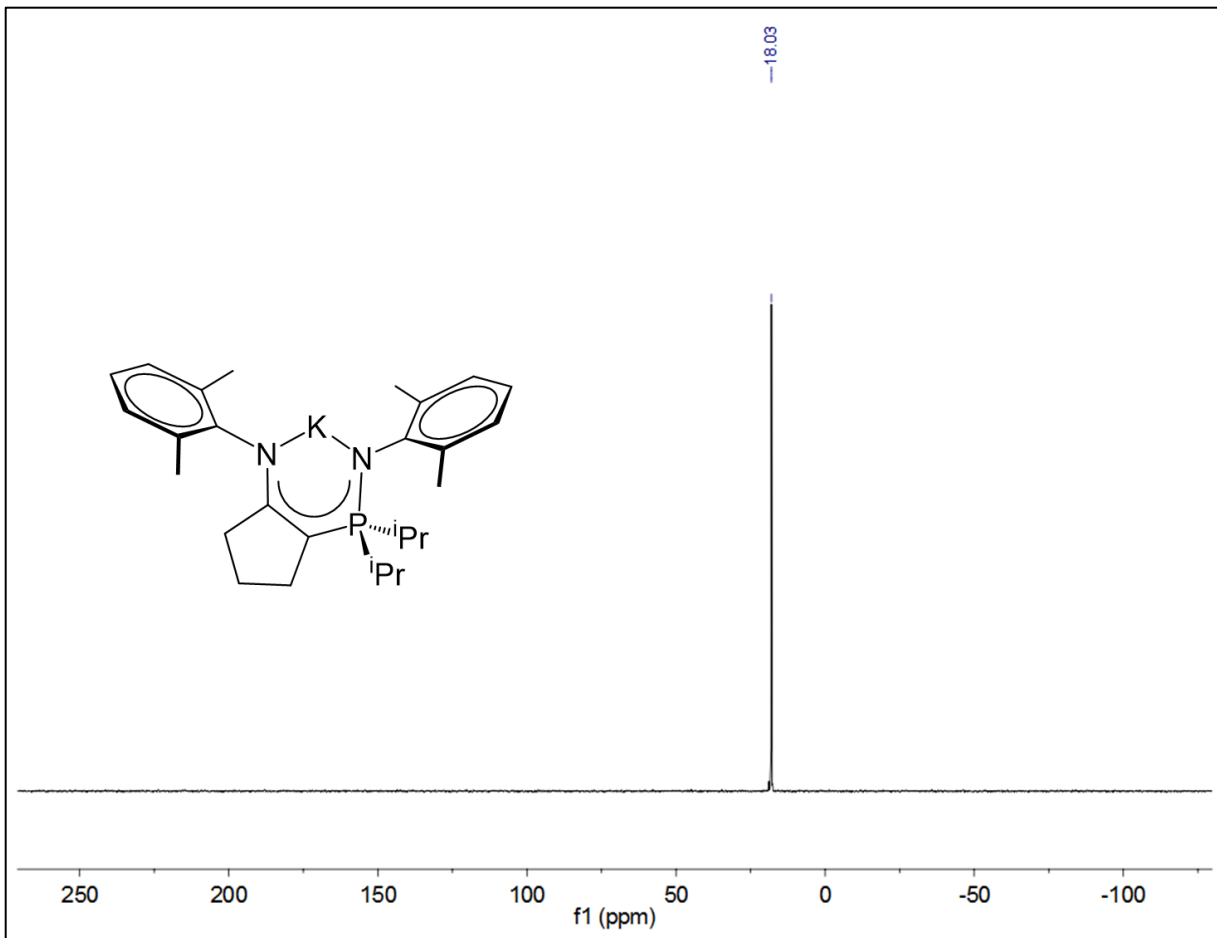


Figure S16: $^{31}\text{P}\{\text{H}\}$ NMR spectrum for $[{}^{\text{CY}5}\text{NpN}^{\text{DMP,DMP}}]\text{K}(\text{THF})_{0.25}$ **3b**
(161 MHz, d_6 -benzene, 298 K).

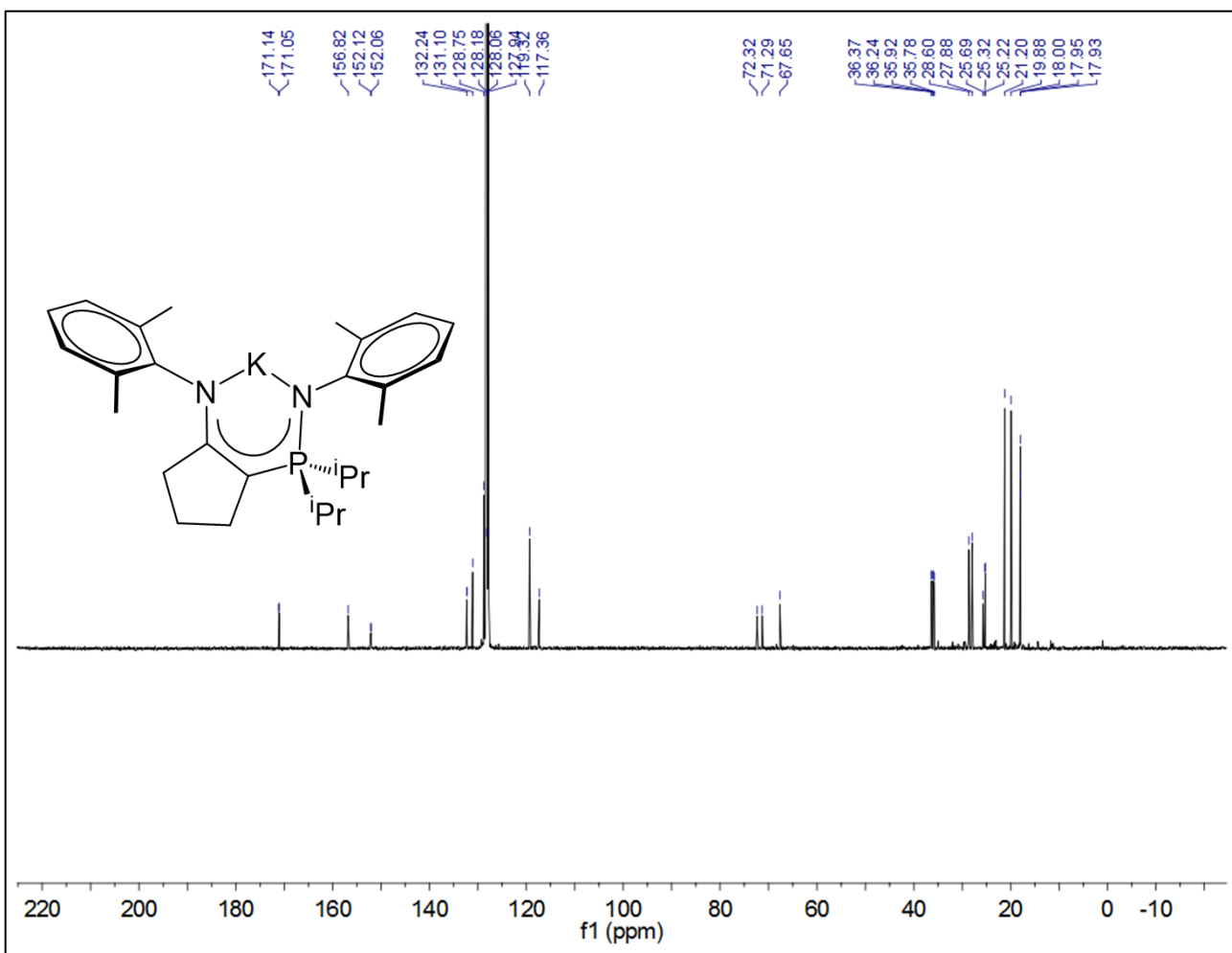


Figure S17: $^{13}\text{C}\{\text{H}\}$ NMR spectrum for $[\text{CY}^5\text{NpN}^{\text{DMP},\text{DMP}}]\text{K}(\text{THF})_{0.25}$ **3b**
(101 MHz, d_6 -benzene, 298 K).

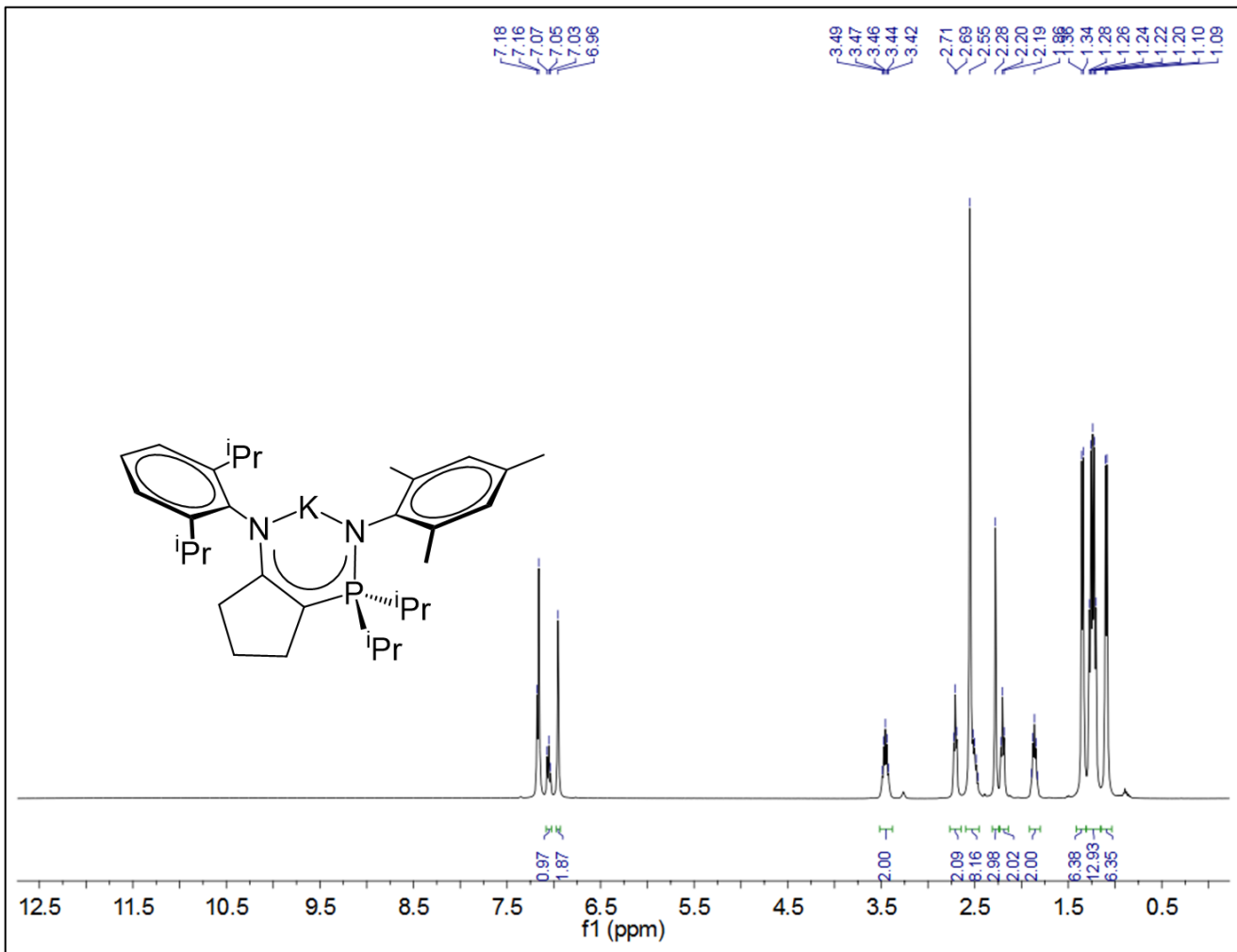


Figure S18: ^1H NMR spectrum for $[\text{CY}^5\text{NpN}^{\text{DIPP},\text{Mes}}]\text{K } 3\text{c}$ (400 MHz, d_6 -benzene, 298 K).

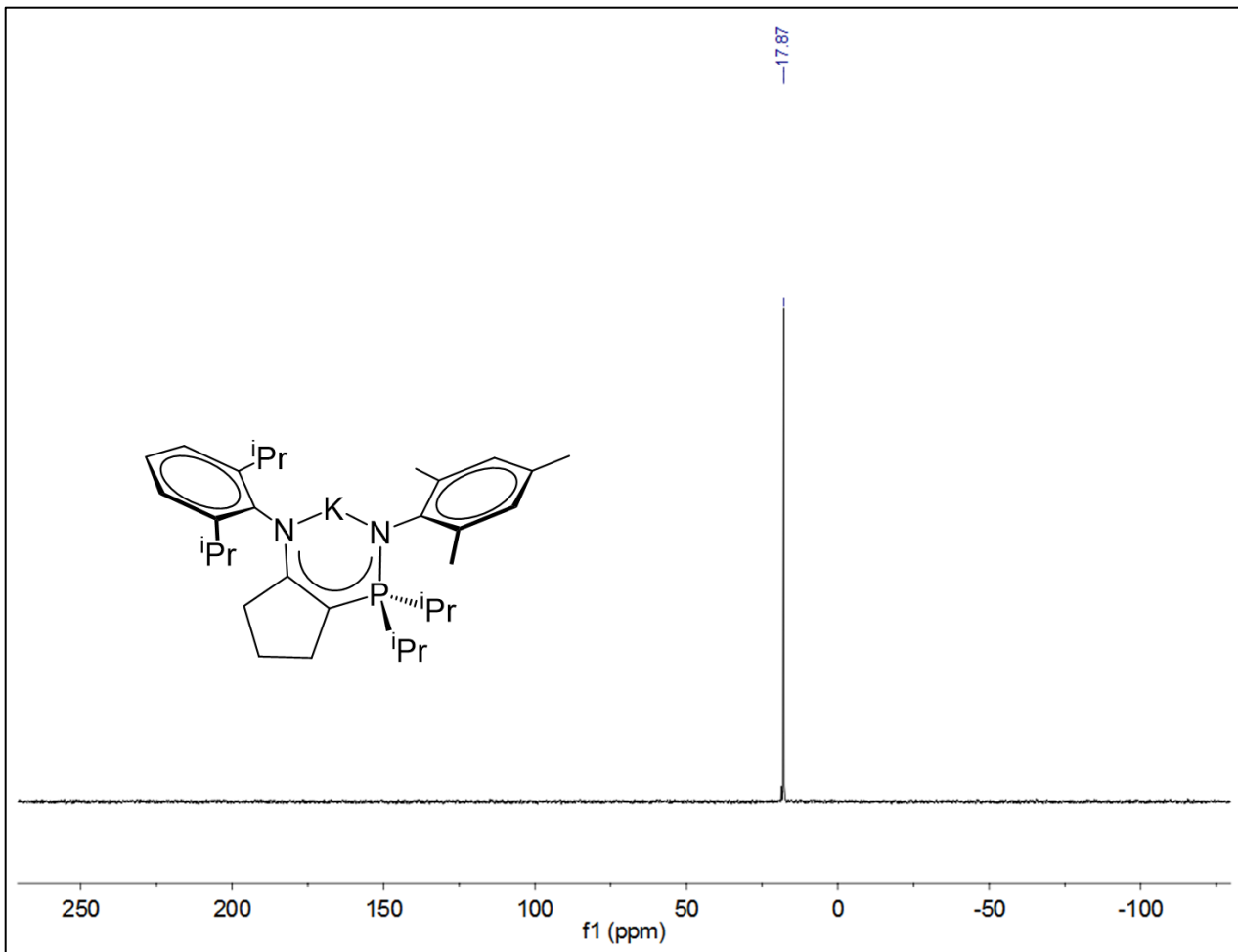


Figure S19: $^{31}\text{P}\{\text{H}\}$ NMR spectrum for $[\text{CY5NpN}^{\text{DIPP},\text{Mes}}]\text{K 3c}$ (121 MHz, d_6 -benzene, 298 K).

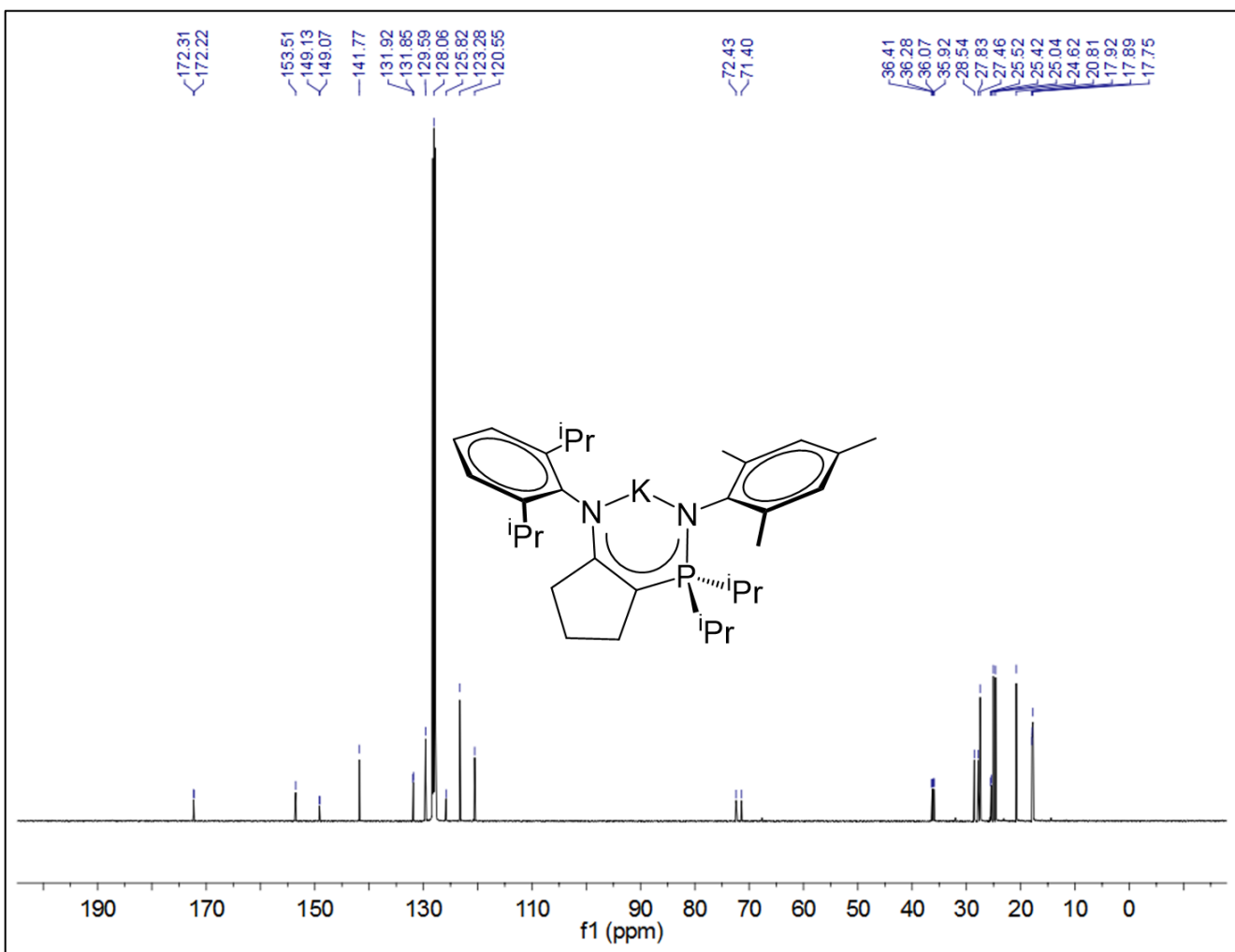


Figure S20: $^{13}\text{C}\{\text{H}\}$ NMR spectrum for $[\text{CY5NpN}^{\text{DIPP},\text{Mes}}\text{K}] \mathbf{3c}$ (101 MHz, d_6 -benzene, 298 K).

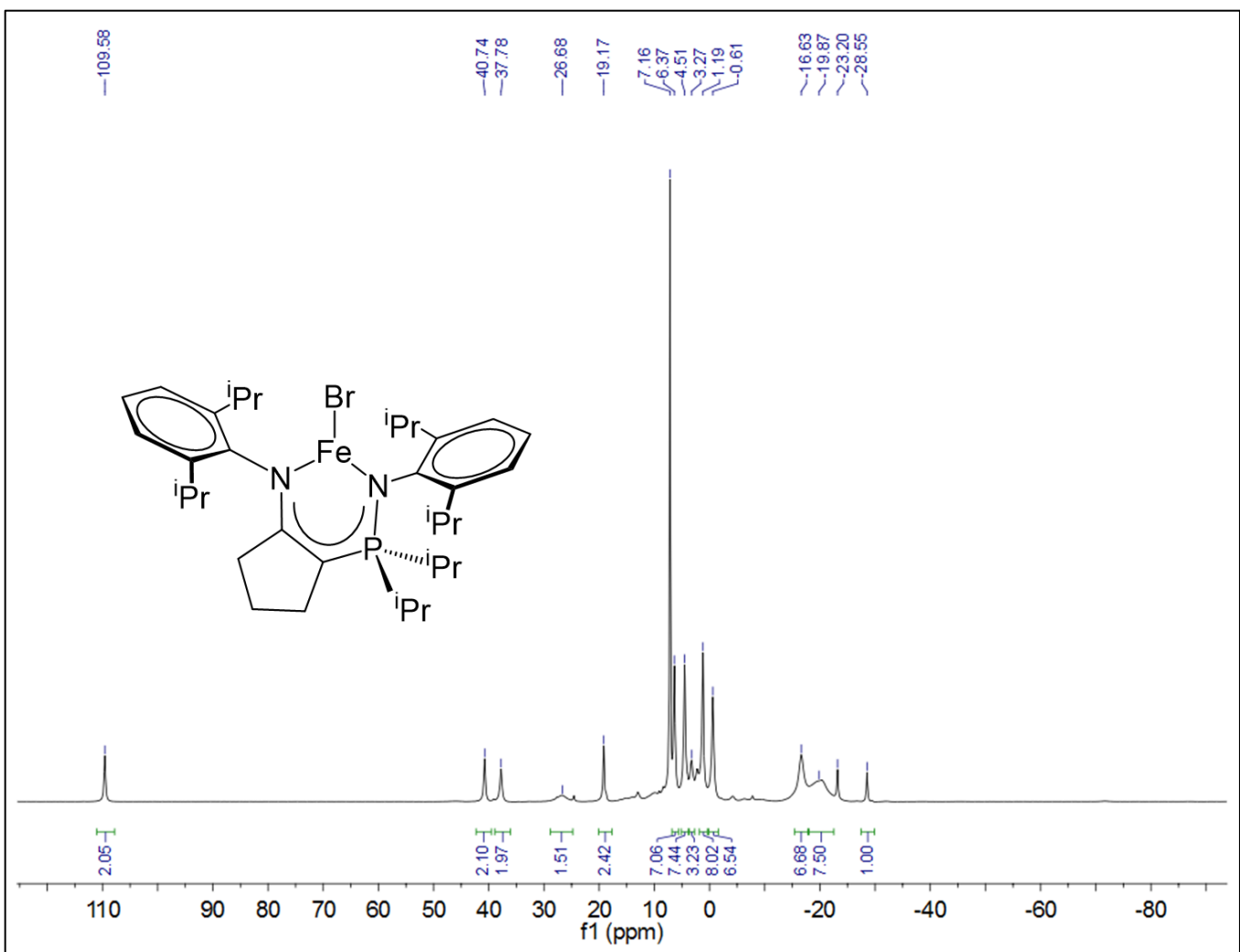


Figure S21: ^1H NMR spectrum for $[\text{CY}^5\text{NpN}^{\text{DIPP},\text{DIPP}}]\text{FeBr}$ 4a (300 MHz, d_6 -benzene, 298 K).

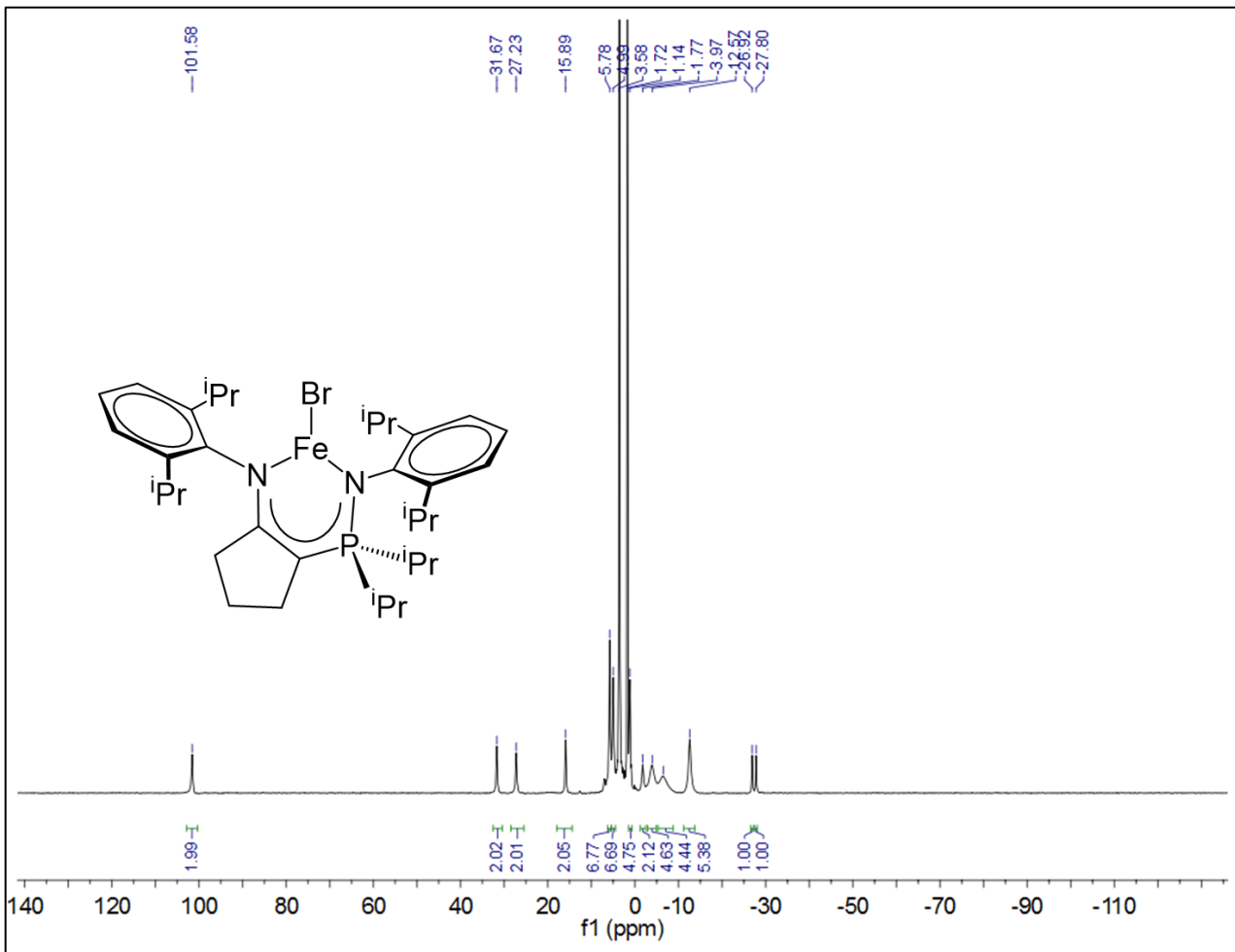
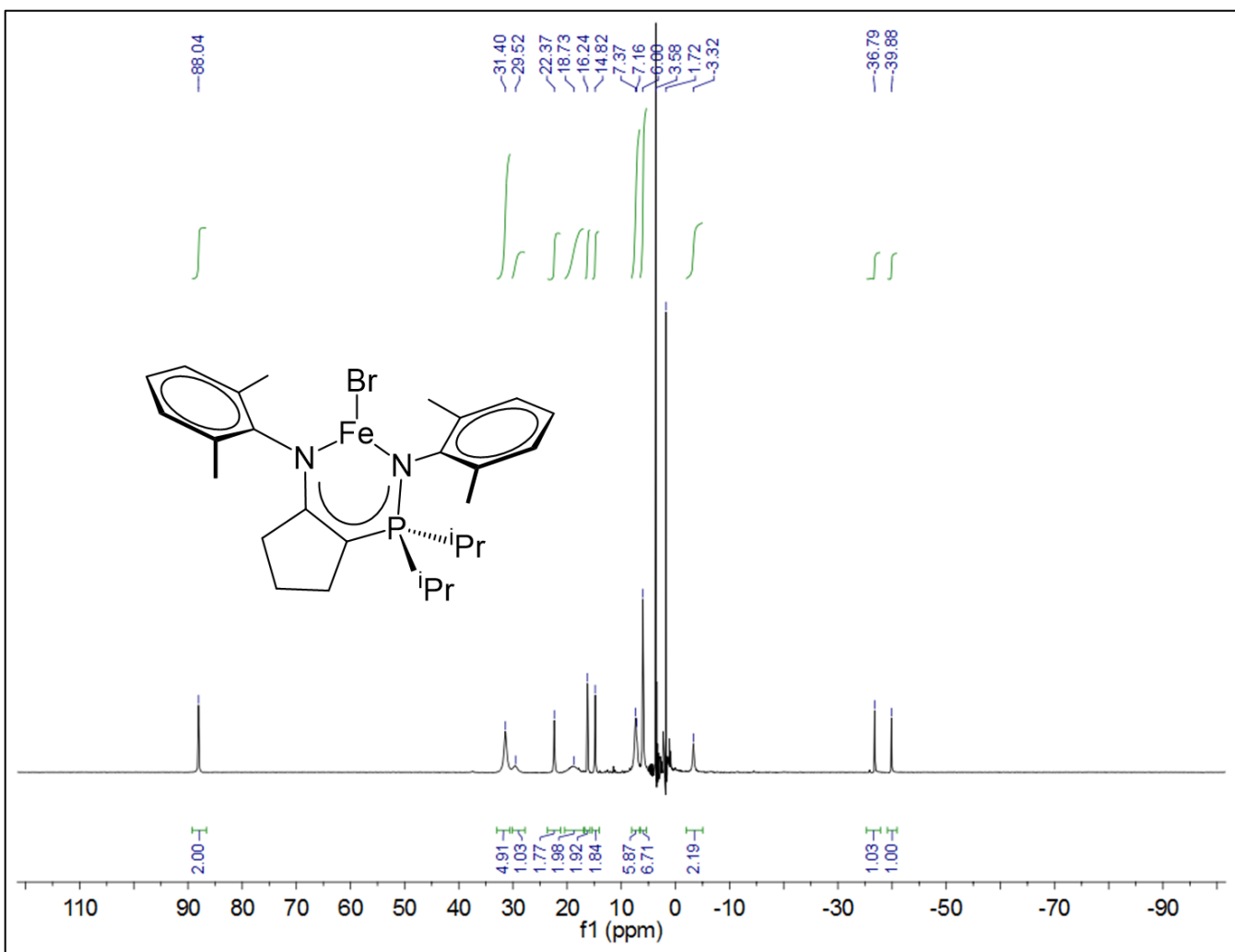


Figure S22: ^1H NMR spectrum for $[\text{CY}^5\text{NpN}^{\text{DIPP},\text{DIPP}}]\text{FeBr}$ **4a** (400 MHz, d_8 -THF, 298 K).



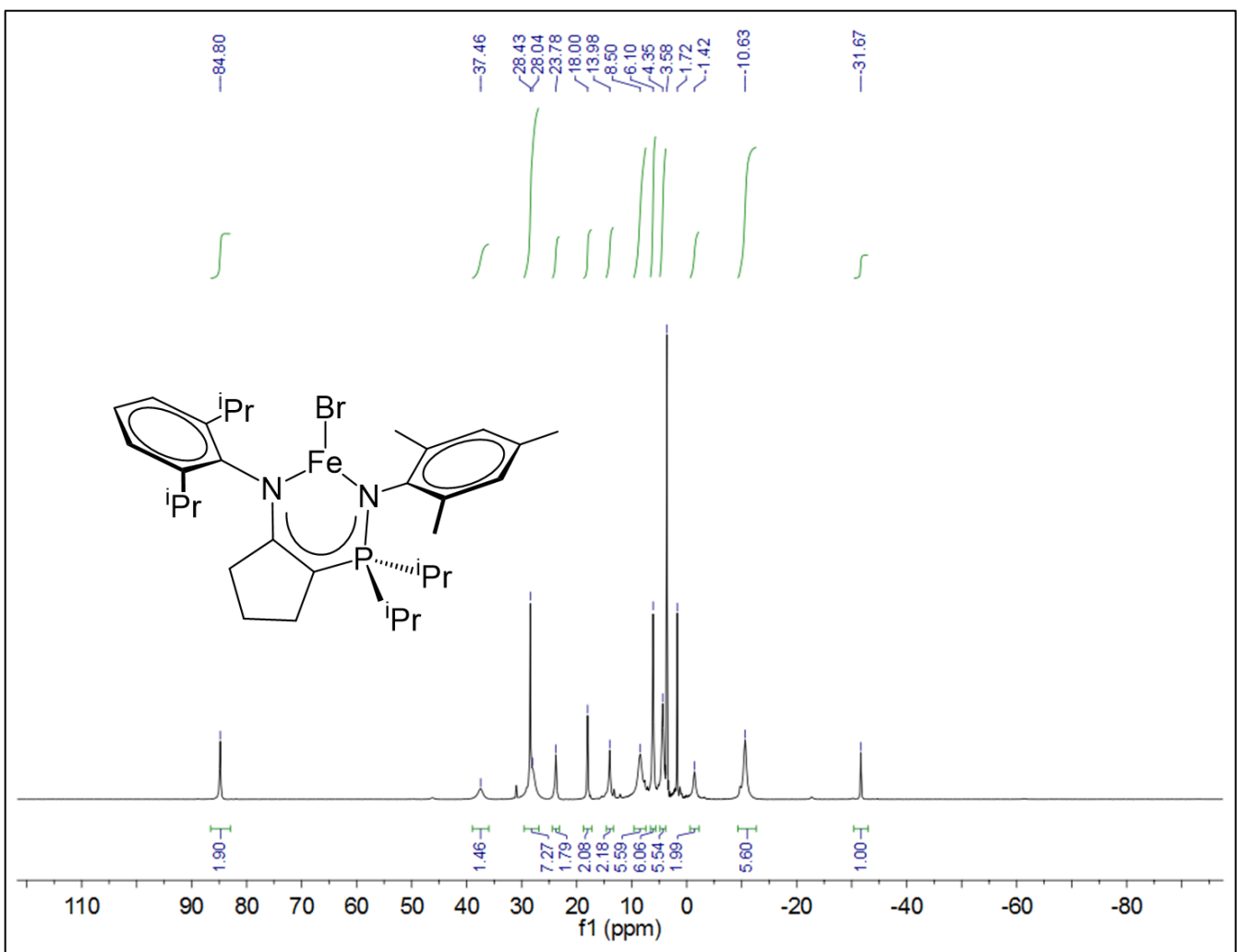


Figure S24: ¹H NMR spectrum for (^{CYP}NpN^{DIPP,Mes})FeBr **5c** (300 MHz, *d*₈-THF, 298 K).

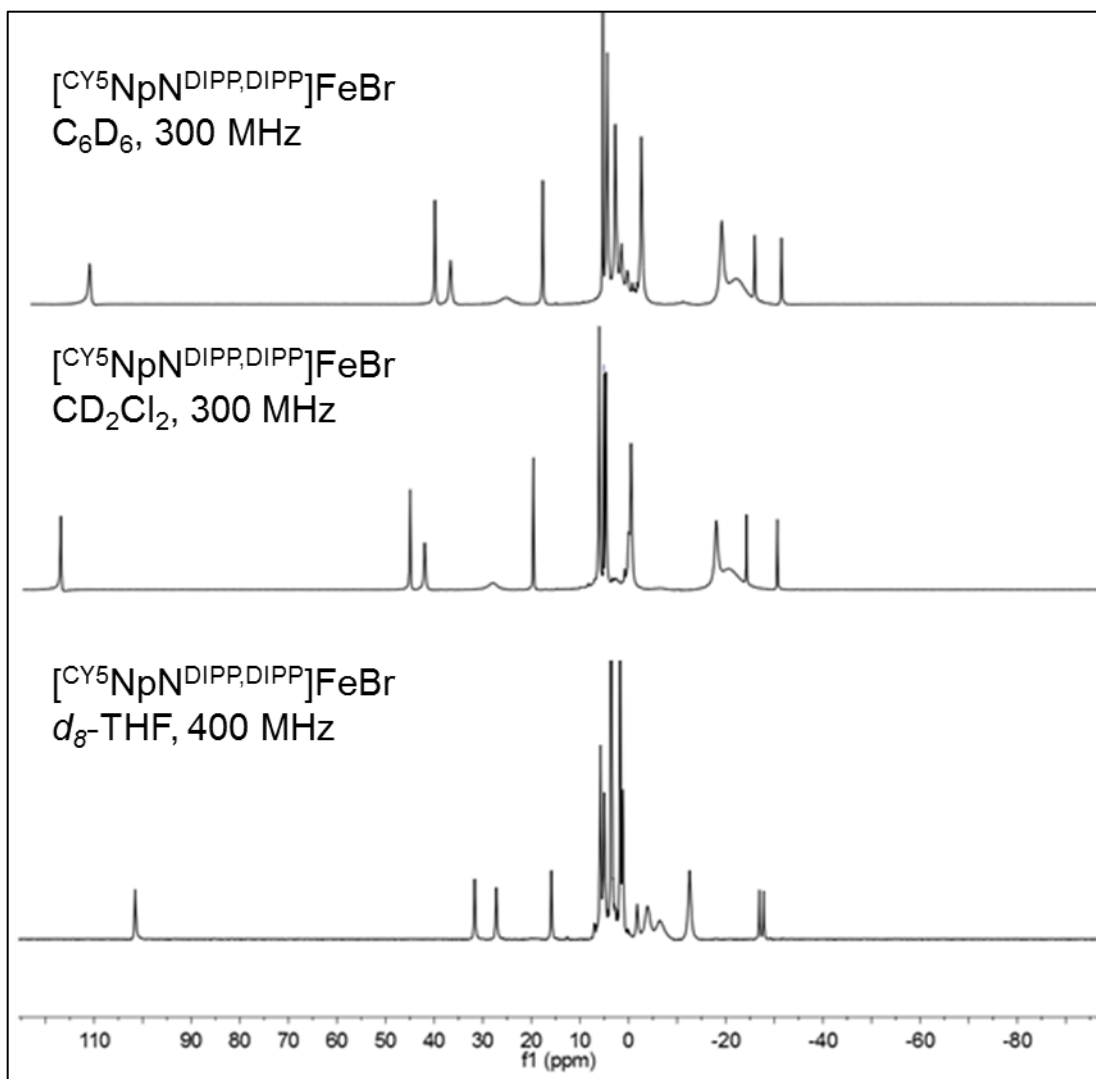


Figure S25: ^1H NMR spectra for $[\text{CY}^5\text{NpN}^{\text{DIPPO},\text{DIPPO}}]\text{FeBr}$ **4a** in d_6 -benzene (top), d_2 -DCM (middle), and d_8 -THF (bottom).

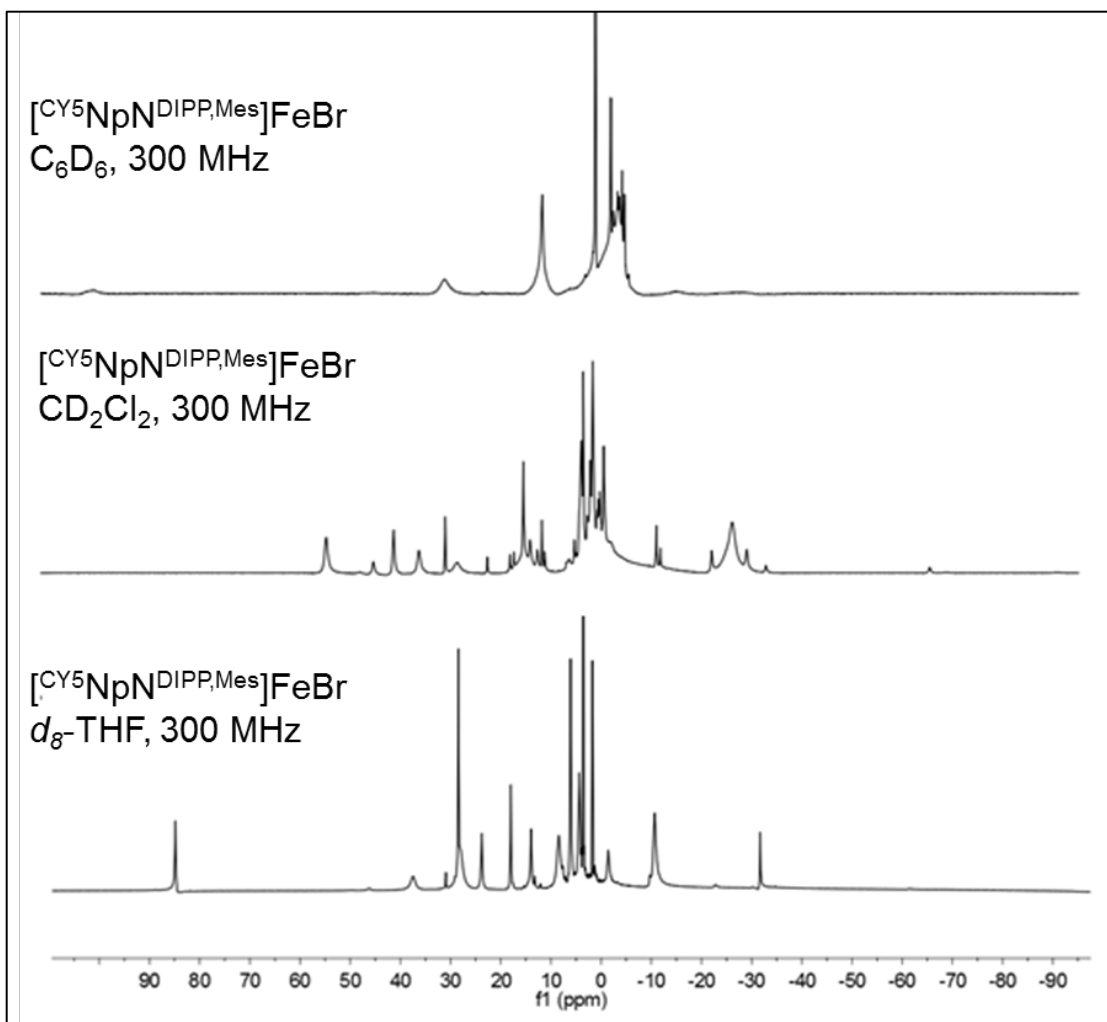


Figure S26: ¹H NMR spectra for $[\text{CY}^5\text{NpN}^{\text{DIPP},\text{Mes}}]\text{FeBr}$ 4c in d_6 -benzene (top), d_2 -DCM, (middle) and d_8 -THF (bottom).

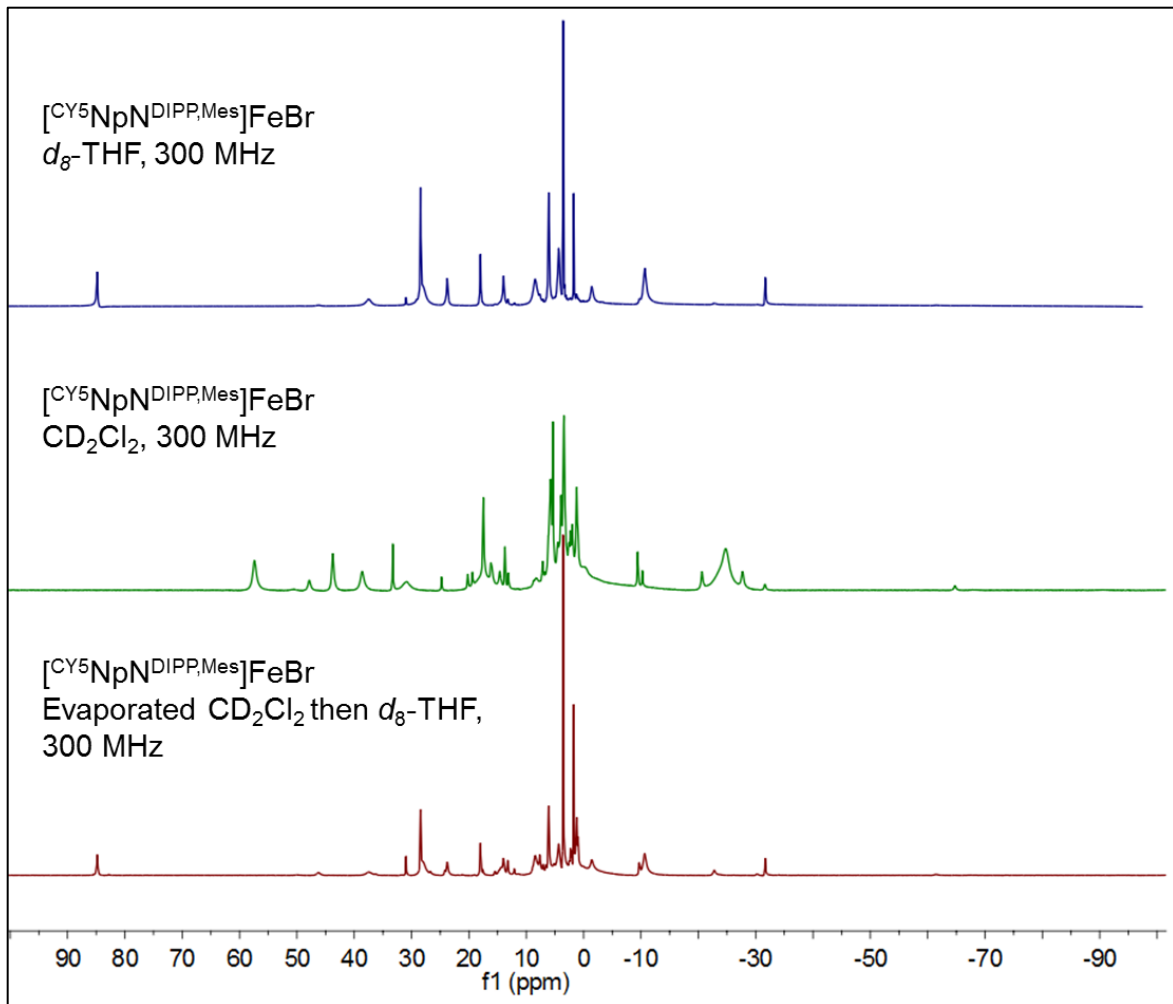


Figure S27: ^1H NMR spectra for $[\text{CY}^5\text{NpN}^{\text{DIPP},\text{Mes}}]\text{FeBr}$ **4c** in $d_8\text{-THF}$ (top), $d_2\text{-DCM}$ (middle), and the $d_2\text{-DCM}$ sample which was evaporated under vacuum and redissolved in $d_8\text{-THF}$ (bottom).

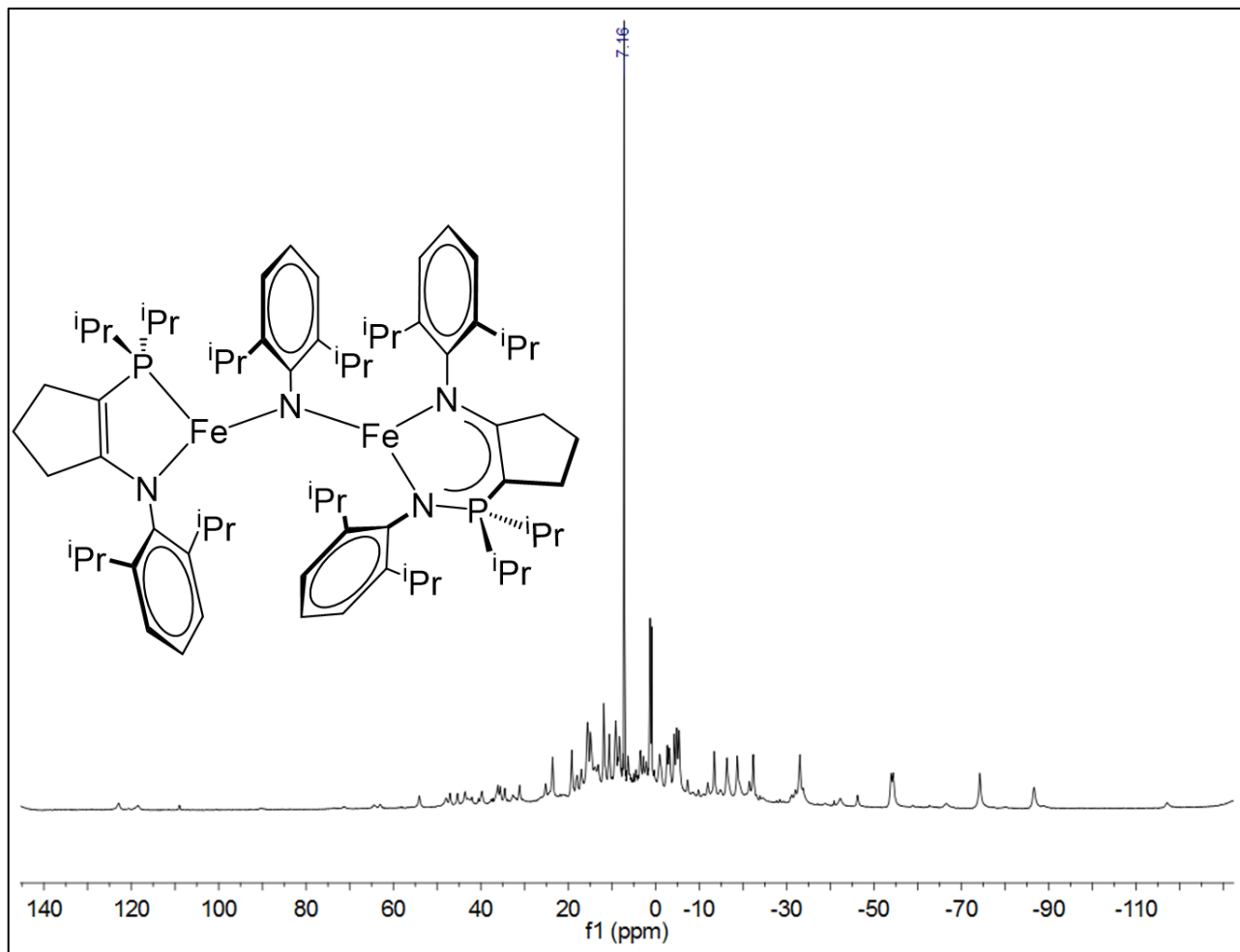


Figure S28: ^1H NMR spectrum for $[\text{CY}^5\text{NpN}^{\text{DIPP},\text{DIPP}}]\text{Fe}(\mu\text{-N-DIPP})\text{Fe}[[\text{CY}^5\text{NP}^{\text{DIPP}}]]$ **6** (300 MHz, d_6 -benzene, 298 K).

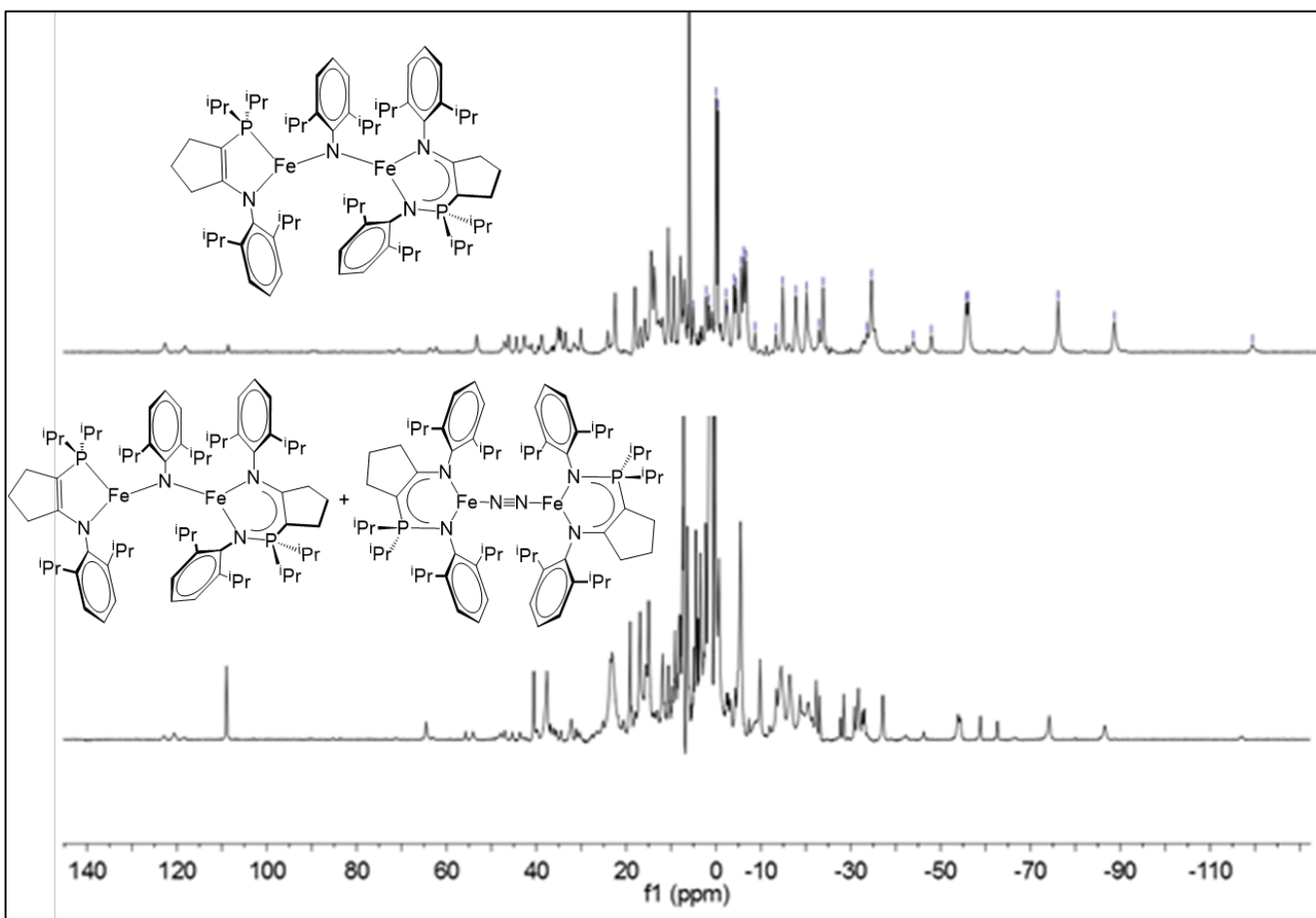


Figure S29: ¹H NMR spectra for the mixture of products obtained from the reduction of (^{CYP}NpN^{DIPP,DIPP})FeBr **5a** with KC₈ (bottom) and ^{CYP}NpNFe(μ -N-DIPP)FeNP^{CYP} **11** (top) (300 MHz, *d*₆-benzene, 298 K).

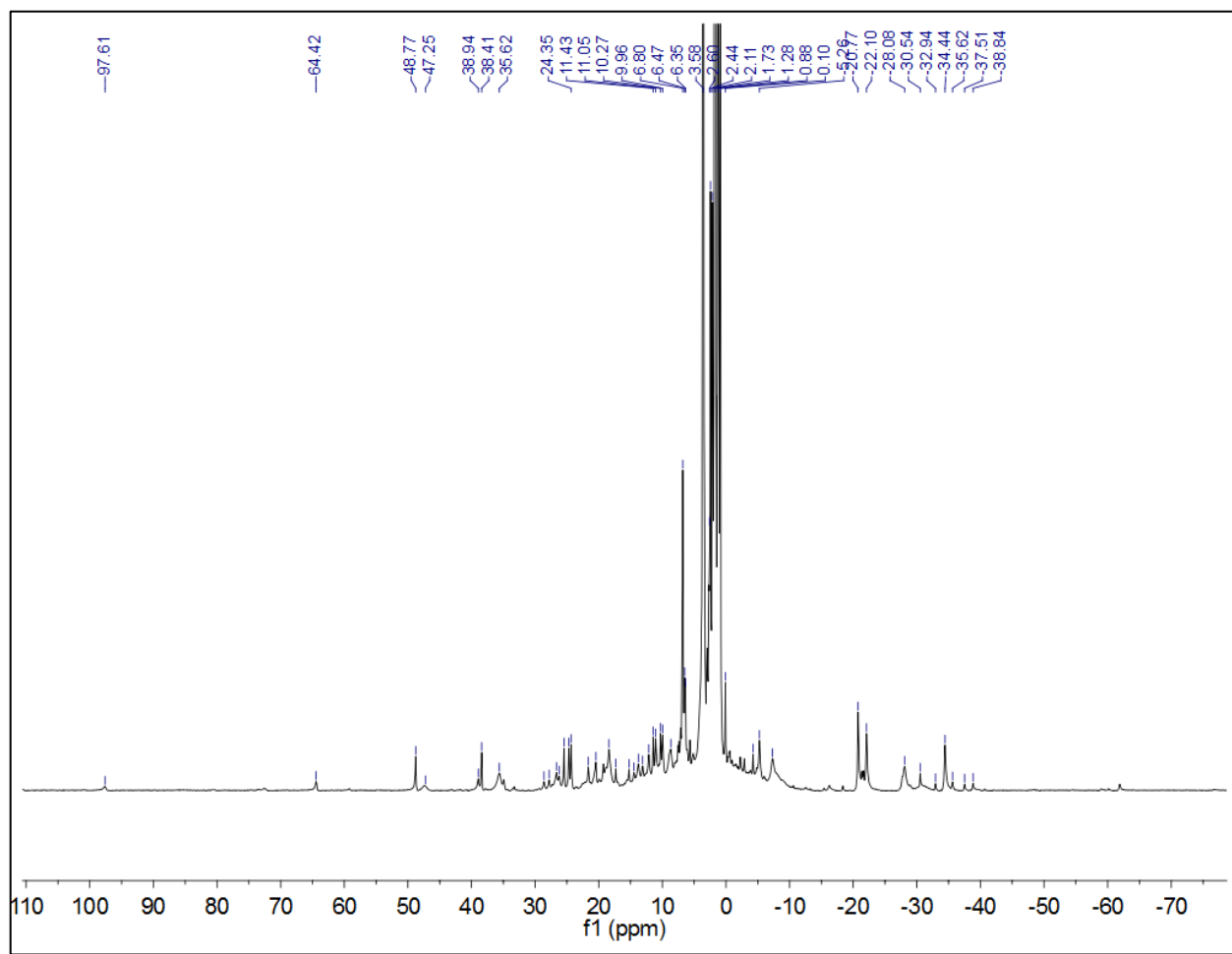


Figure S30: ¹H NMR for product mixture that a crystal of (^{CY5}NpN^{DMP,DMP})^{[^{CY5}NP] Fe) (5b) was picked from (400 MHz, *d*₈-THF, 298 K).}

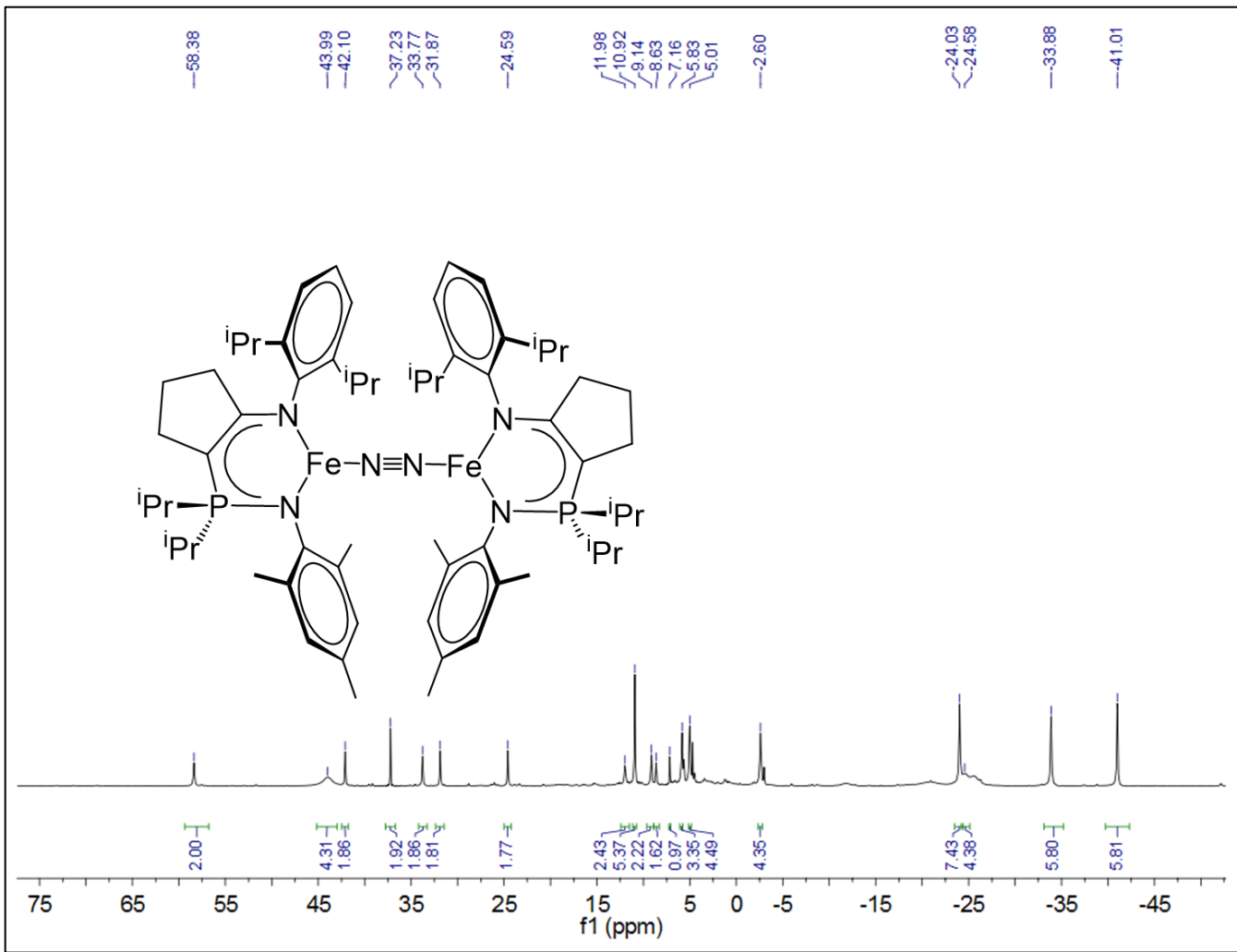


Figure S31: ¹H NMR spectrum for $[(\text{CYPNpN}^{\text{DIPP},\text{Mes}})\text{Fe}]_2(\mu\text{-N}_2)$ (300 MHz, d_6 -benzene, 298 K).

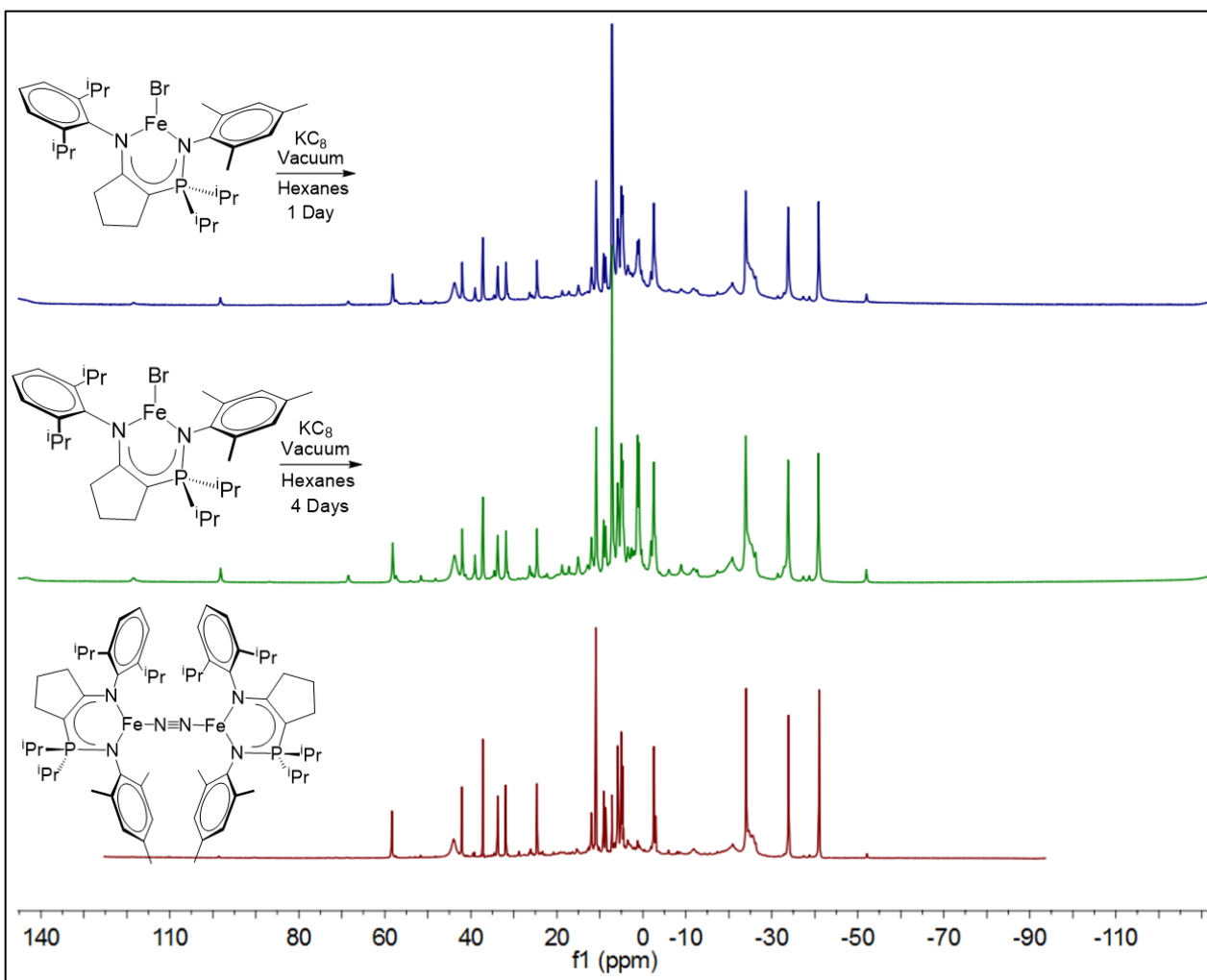


Figure S32: ¹H NMR spectra for the reduction of **5c** under vacuum for 1 day (top) the reduction of **5c** under vacuum for 4 days (middle), and the spectrum for $[({}^{\text{CYP}}\text{NpN}^{\text{DIPP},\text{Mes}})\text{Fe}]_2(\mu\text{-N}_2)$ (bottom). Impurities denoted with (*). (300 MHz, *d*₆-benzene, 298 K).

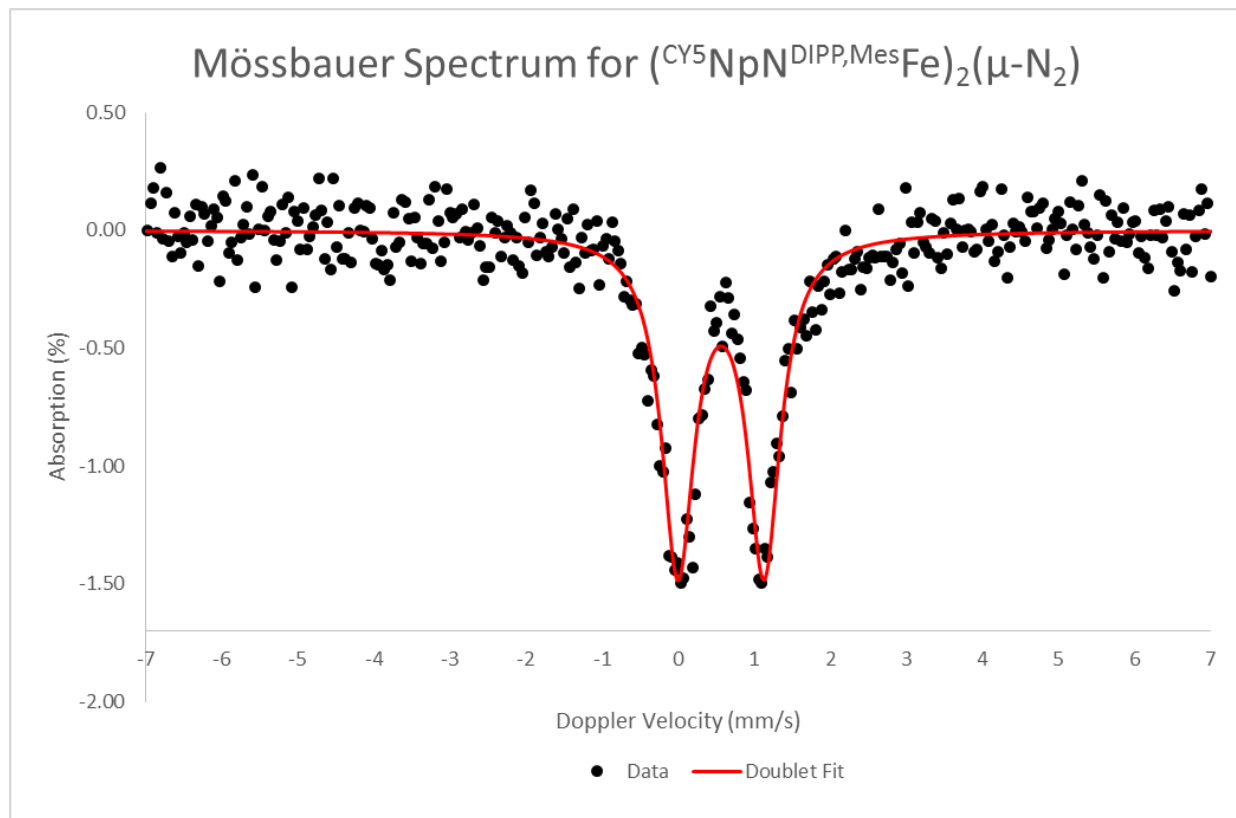


Figure S33: Zero-field ⁵⁷Fe Mössbauer spectra for powdered samples of [^{CYP}NpN^{DIPP,Mes}Fe]₂(μ-N₂) **5c** obtained at 295 K. The parameters used for the fit of **5c** (red line) were an isomer shift of (δ) 0.56 mm/sec and a quadrupole splitting (ΔE_Q) of 1.14 mm/sec.